(BL-1B)

# Vacuum Ultraviolet Reflection Spectra of Sulfide Glasses

Hiromichi Takebe

*Department of Applied Science for Electronics and Materials,*
*Graduate School of Engineering Sciences,*
*Kyushu University, Fukuoka 816-8580*

Sulfide glasses are prospective candidates for new fiber lasers and non-linear optical switches in near infrared and infrared regions. We have been studying Ge-S and $Ga_2S_3$-based glasses as alternatives of As-S glass with toxicity. All of sulfide glasses have high refractive indexes over 2 in the visible and near infrared regions [1]. The refractive index are related to the reflection properties of glass in the ultraviolet vacuum region. There are, however, to my knowledge, no reports on the reflection spectra of sulfide glasses except for As-S glass. In this work the reflection spectra of As-S, $Ga_2S_3$, and Ge-S based glasses were measured.

Spectral measurements were performed using a $As_{40}S_{60}$ glass for comparison, a typical $Ga_2S_3$-based glass with a composition of $70Ga_2S_3 \cdot 30La_2S_3$ , and a series of Ge-S glasses with various S concentrations. Figure 1 shows the representative reflection spectra of sulfide glasses. The reflection bands due to the glass networks of M-S (M = As, Ga, Ge) are observed at 100 - 500 nm. The peaks of the reflection bands due to sulfur ions are located at longer wavelengths than those of the bands due to oxygen ions in oxide glasses [2]. These positions of the reflection bands correspond to the characteristics of refractive index dispersion; sulfide glasses have higher refractive index and dispersion than oxide glasses. Refractive indexes $n_d$ of the sulfide glasses are 2.650 for $As_{40}S_{60}$, 2.493 for $70Ga_2S_3 \cdot 30La_2S_3$ (GLS), and 2.156 for $Ge_{33}S_{67}$. The highest $n_d$ of $As_2S_3$ glass is related to the relatively-longer resonance wavelength of the reflection band located at 300 - 400 nm, compared with those of GLS and Ge-S glasses. GLS glass has relatively-high refractive indexes and low dispersion characteristics in sulfide glasses [3]. This feature of GLS glass corresponds to the higher reflection intensity of the band in spite of its shorter wavelength by comparison with $As_{40}S_{60}$ glass.

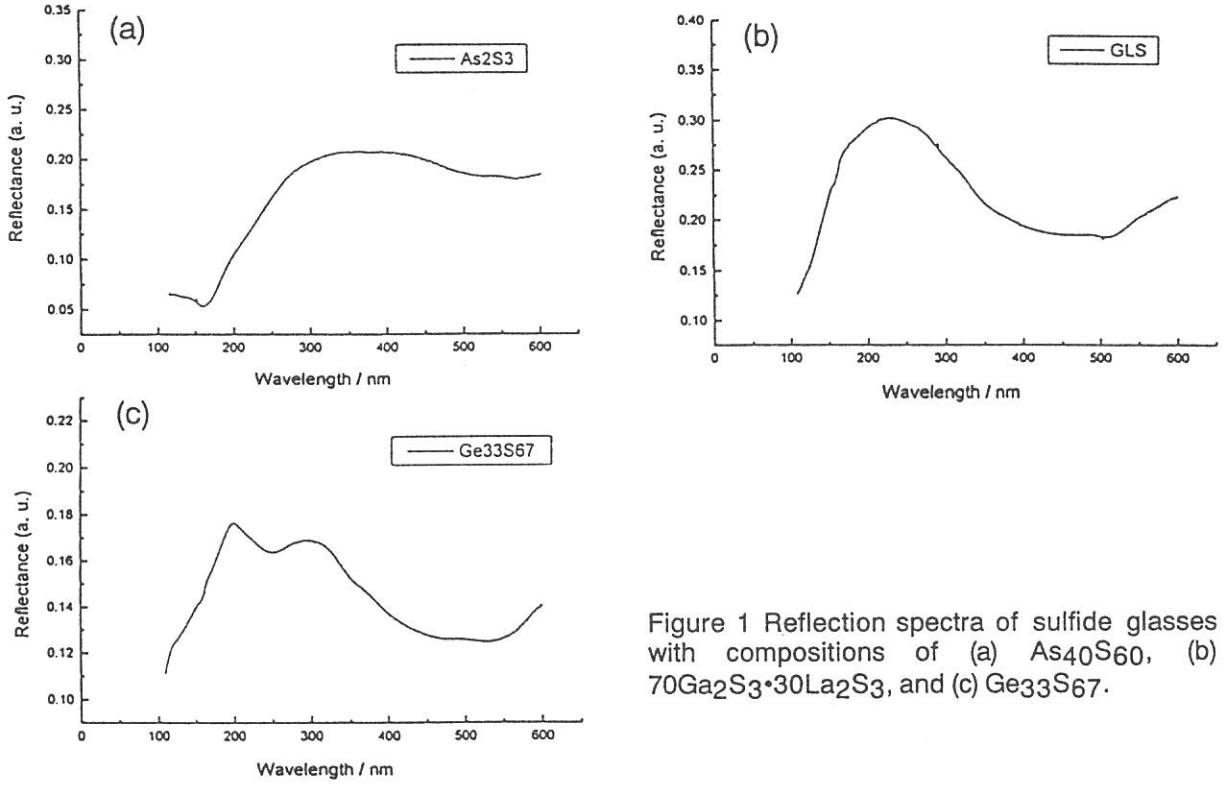


Figure 1 Reflection spectra of sulfide glasses with compositions of (a) $As_{40}S_{60}$, (b) $70Ga_2S_3 \cdot 30La_2S_3$, and (c) $Ge_{33}S_{67}$.

[1] H. Takebe, EMIS DATAREVIEWS SERIES No. 22, IEE (1998), pp. 294-297.
[2] T. Mito, S. Fujino, H. Takebe, K. Morinaga, S. Todoroki, S. Sakaguchi, J. Non-Cryst. Solids, 210 (1997) 155-162.
[3] H. Yayama, S. Fujino, K. Morinaga, H. Takebe, D. W. Hewak, and D. N. Payne, J. Non-Cryst. Solids (1998).

(BL1B)

# Optical properties of cerium-doped LiCAF and LiSAF crystals for vacuum ultraviolet optical materials

Masahiro SAKAI, Zhenlin LIU[a], Hideyuki OHTAKE[a], Nobuhiko SARUKURA[a], Yusaburo SEGAWA[b], Yoshikazu MIYAZAWA[c], Kiyoshi SHIMAMURA[d], Sonia L. BALDOCHI[d], Kenji NAKANO[d], Na MUJILATU[d], and Tsuguo FUKUDA[d]

*Research Center for Molecular Materials,*
*Institute for Molecular Science (IMS), Myodaiji, Okazaki 444-8585, Japan*
[a] *Laser Center for Molecular Science,*
*Institute for Molecular Science (IMS), Myodaiji, Okazaki 444-8585, Japan*
[b] *Photodynamics Research Center, The Institute of Physical and Chemical Research (RIKEN), Nagamachi Koeji 19-1399, Aoba-ku, Sendai, Miyagi 980-0868, Japan*
[c] *Research and Development Department, Optron Inc.*
*Hakusan 7-5-16, Toride, Ibaraki 302-0032, Japan*
[d] *Institute for Materials Research, Tohoku University,*
*Katahira 2-1-1, Aoba-ku, Sendai 980-8577, Japan*

Various new fluoride crystals have been developed as the host crystals for new solid-state tunable ultraviolet and infrared laser materials. Among them, $LiCaAlF_6$ (LiCAF) and $LiSrAlF_6$ (LiSAF) are the successful material for Chromium [1] or Cerium [2], doping. For Cerium doping in particular, Ce:LiCAF and Ce:LiSAF are attractive solid-state lasers with their practical tuning region from 288 to 315 nm [3]. In spite of similar tunability and laser efficiency, Ce:LiCAF is even more attractive because of its reduced solarization effects compared with Ce:LiSAF. However, the reason for this difference has not been studied well, and to further improve laser performance, spectroscopic studies of these materials will be necessary, including accurate band-gap measurement. In addition, optical material for the ultraviolet and vacuum ultraviolet region has become much more important for the deep ultraviolet lithographic technology required for the semiconductor processing technology of the next century and vacuum ultraviolet spectroscopy using synchrotron orbital radiation.

Crystals of Ce:LiCAF, Ce:LiSAF and LiF were grown by the CZ method. The preparation of raw powder material under a reactive atmosphere was the same for all of these fluoride crystals. All crystals ware about 1-mm thick. To measure the transmission spectra of various fluoride materials at room temperature, an experiment was performed at the beam line BL1B of UVSOR using a 1-m focal-length Seya-Namioka monochromator. The transmission at wavelengths from 100 to 200 nm was detected by a photo multiplier (Hamamatsu R105). All of the fluoride samples were mounted on sample holders separately, and introduced into a sample chamber. Figure 1 shows the transmission spectrum of various fluoride samples. The transmission edge of our LiF was slightly longer than that (102 nm) of the very best sample ever reported in ref. 4. The transmission edge of LiCAF was measured to be 112 nm and that of LiSAF was 116 nm. This difference may explain the solarization free nature of Ce:LiCAF compared with Ce:LiSAF. The absorption at around 125 nm might be attributed to the color center or impurity. Therefore, after the crystal quality is improved, this absorption should disappear. The problems of the commonly used optical materials for the ultraviolet and vacuum ultraviolet region such as LiF are the limitation of transmission wavelength, solarization of the material with irradiation of high power ultraviolet light, and the difficulty of material processing and polishing due to the cleavage or the hydroscopic nature. LiCAF does not have the cleavage or hydroscopic characteristics [5]. Therefore, LiCAF will be a suitable optical material for the ultraviolet and vacuum ultraviolet region, becoming much more important for the next generation lithographic technology.

In conclusion, superior transmission characteristics of $LiCaAlF_6$ (LiCAF) down to 112 nm were found for the first time. From the transparent wavelength shorter than that of conventional LiF, the non hydroscopic nature of LiCAF, and the better mechanical properties compared with LiF, LiCAF was shown to be an ideal optical material for the vacuum ultraviolet region.

The authors are grateful to Mr. M. Hasumoto and Prof. M, Kamada for their experimental support.

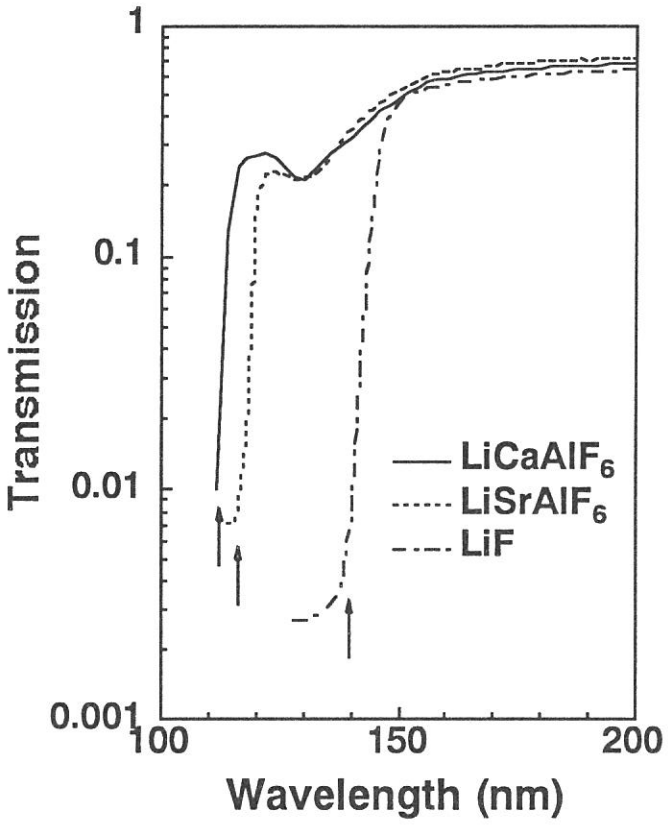


Fig. 1. Transmission characteristics of LiCAF, LiSAF and LiF at room temperature. The arrows show transmission edge wavelengths of various fluoride crystals. According this figure, transmission edge of LiCAF, LiSAF and LiF were 112 nm, 116 nm and 136 nm, respectively.

References

[1] S. A. Payne, L. L. Chase, H. W. Newkirk, L. K. Smith, and W. F. Krupke, IEEE J. Quant. Electron. 24, 2243 (1988); S. A. Payne, L. L. Chase, L. K. Smith, W. L. Kway, and H. W. Newkirk, J Appl. Phys. 66, 1051 (1989).

[2] M. A. Dubinskii, V. V. Semashko, A. K. Naumov, R. Y. Abdulsabirov, and S. L. Korableva, OSA proceedings on Advanced Solid-State Lasers, A. A. Pinto and T. Y. Fan, eds. (OSA 1993), vol. 15, 195; M. A. Dubinskii, V. V. Semashko, A. K. Naumov, et al. J. Mod. Opt., 40, 1, (1993); J. F. Pinto, G. H. Rosenblatt, L. Esterowitz, and G. J. Quarles, Electron. Lett. 30, 240 (1994); C. D. Marshall, S. A. Payne, J. A. Speth, W. F. Krupke, G. J. Quarles, V. Castillo, and B. H. T. Chai, J. Opt. Soc. Am. B. 11, 2054 (1994).

[3] See, for example, Z. Liu, S. Izumida, H. Ohtake, N. Sarukura, K. Shimamura,, N. Mujilatu , S. Baldochi, and T. Fukuda, Jpn. J. Appl. Phys., 37, L1318 (1998)

[4] E. D. Palik, "Handbook of Optical Constants of Solids", Academic Press, Inc. 1985.

[5] M. J. Weber, "Handbook of Laser Science and Technology", Supplement 2, CRC Press, Inc., 1994.

# (BL1B) VUV Excited Photoluminescence in Multilayer Structures of Alkali Earth Fluorides

Arisato Ejiri, Akira Urasaki, Sinobu Kinjou, Tetsuya Tamaki and Asamitsu Taminato

*Dept.of Science Education, College of Education, Univ. of the Ryukyus. Okinawa 903-0219 Japan.*

It is well known that STE(self trapped exciton) luminescence in alkali earth fluorides ($CaF_2$, $SrF_2$, $BaF_2$) crystal can be strongly observed even at room temperature.[1] VUV excited luminescence in multilayer structures with 5 periods of LiF(200Å)-$CaF_2$(100Å) and of LiF(200Å)-$BaF_2$(100Å) were previously obseved [2], and a line series of luminescence was found in the former specimen at longer wavelength region than that of the original luminescence in $CaF_2$ crystal.

This phenomena were analyzed in terms of a multimode interference in a cavity made of the multilayer structure.

Present paper will report on the results of the similar measurement of VUV excited luminescence in multilayer structure of LiF-$CaF_2$ nad LiF-$BaF_2$. Sample specimen were deposited on the both of LiF single crystal and of Ag coated LiF single crystal and had compositions with commonly 5 periods in respect of LiF(200Å)-$CaF_2$(100Å), LiF(100Å)-$CaF_2$(50Å), LiF(200Å)-$BaF_2$(100Å), and LiF(100Å)-$BaF_2$(50Å). Typical results of the present measurement are shown in Fig. 1 -Fig. 3. In Fig. 1, STE luminescence spectra excited with 1050 Å light in single crystal specimens $CaF_2$ and $BaF_2$ at room temperature and a low temperature are shown. STE luminescences of these single crystals seem to become very large at the low temperature

In Fig. 2, the luminescence of the multilayer specimen and in Fig. 3, the excitation spectra of the multilayer luminescence are shown.

It is interesing phenomena that the multilayer luminescence at room temperature shows a much larger intensity than that at the low temperature contrarily to the case of the single crystals.

From these experimental studies, it was clearly revealed that the intensity of the multilayer luminescence was enhanced at around 300 nm as an effect of silver coating on the substrate as can be seen in Fig. 2. It should be also noted that the luminescence spectra have a doublet structure in the both of $CaF_2$ multilayer and $BaF_2$ one as can be seen in Fig. 2. This phenomena would be very interesting, because it can be expected that STE state likely confined in the well layer. Structures of the excitation Spectra having a large peak around 10 eV (Fig. 3) are strongly depended on the multilayer compositions.

References

1) A. Ejiri, A. Hatano, and K. Arakaki; UVSOR Act. Rep. 1995 68 (1996)

2) A. Ejiri, E. Chin, A. Urasaki, T. Yonamine and T. Yokozawa; UVSOR Act. Rep. 1997 106 (1998)

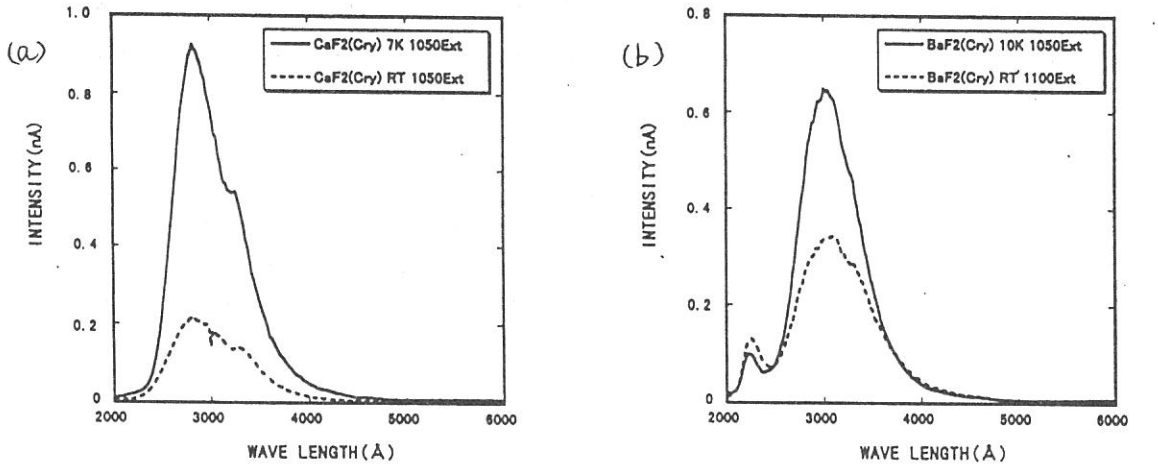


Fig. 1 STE luminescence spectra of (a) $CaF_2$ single crystal excited at 1050 Å and of (b) $BaF_2$ single crystal excited with 1050 Å at 10K and with 1100Å at RT.

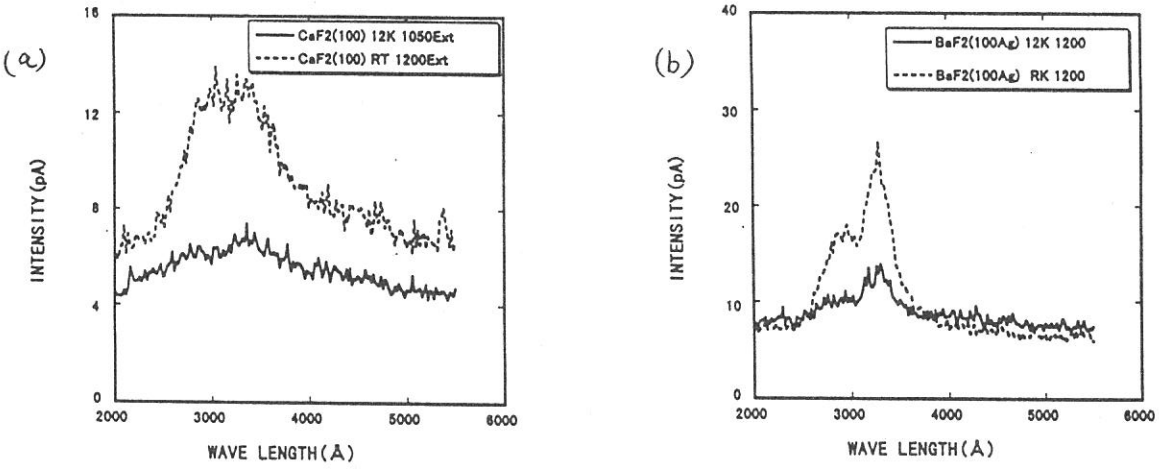


Fig. 2. Luminescence spectra of (a) the $CaF_2$ multilayer with 100 Å well width excited with 1050 Å at 12K and RT, and of (b) the $BaF_2$ multilayer on the Ag coated substrate.

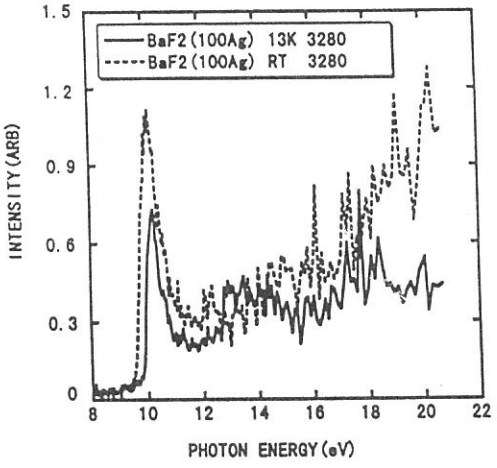


Fig. 3 Excitation spectra of the $BaF_2$ multilayer luminescence of 3280Å at RT and 13K.

(BL1B)

# Two-Photon Spectroscopy of Excitons in $CaF_2$ by Using Synchrotron Radiation and Laser

Toru TSUJIBAYASHI[A], Masayuki WATANABE[B], Osamu ARIMOTO[C], Hiroshi NAGASAKI[C], Minoru ITOH[D], Jun-ichi MURAKAMI[D], Yoshizumi BOKUMOTO[D], Syunsuke NAKANISHI[E], Hiroshi ITOH[E], Shuji ASAKA[F], and Masao KAMADA[G]

[A]*Department of Physics, Osaka Dental University, Hirakata 573-1121*
[B]*Department of Fundamental Sciences, Kyoto University, Kyoto 606-8501*
[C]*Department of Physics, Okayama University, Okayama 700-8530*
[D]*Department of Electrical & Electronic Engineering, Shinshu University, Nagano 380-8553*
[E]*Department of Advanced Materials Science, Kagawa University, Takamatsu 760-8526*
[F]*Equipment Development Center, Institute for Molecular Science, Okazaki 444-8585*
[G]*UVSOR Facility, Institute for Molecular Science, Okazaki 444-8585*

Two-photon spectroscopy (TPS) is an important technique in optical measurements for investigation of electronic structures in condensed matters because of the difference in the parity-selection rules between one- and two-photon absorption transitions. The transition probability of two-photon absorption is much lower than that of one-photon absorption. Therefore, intense light from high-power lasers has been used for TPS. The restriction of laser wavelengths prevents TPS from being applied to wide-band gap materials.

Synchrotron radiation (SR) is one of the most important light sources since it provides continuous distribution in a wide energy range from X-ray to infrared. It is an exciting project to develop a novel technique of TPS using SR and laser, since the combination of the wide spectral range of SR and the high-power of lasers will give us fruitful information of the electronic structures of many materials. We measured the valence excitons of $BaF_2$ by using a time-gated photon counting method [1-5]. The obtained value of the binding energy of the exciton was larger by 50% than that reported in a previous paper [6]. In order to check the previous binding energy in another system, the measurement of the valence exciton in $CaF_2$ was performed. We report the experimental result in this paper.

The crystal of $CaF_2$ has wide band gap of about 12 eV. It is used as a material for optical windows. Under optical excitation around band gap or higher energies, luminescence due to radiative decay of self-trapped excitons (STEs) is observed around 4.4 eV.

The optical system for TPS was constructed at Beam-line 1B. Figure 1 shows a schematic diagram of the apparatus. A cleaved specimen of $CaF_2$ was mounted on a cold finger of a conduction-type cryostat. The SR light

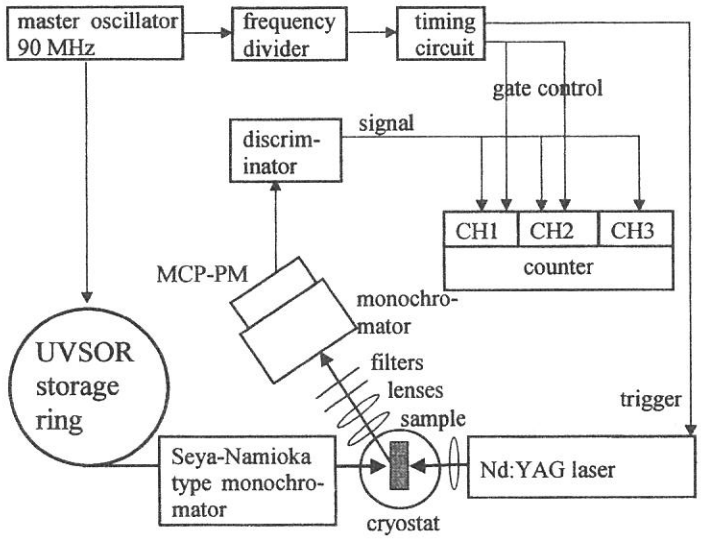


Fig. 1 Schematic diagram of the experimental setup for TPS with SR and laser.

was monochromatized through a 1-m Seya-Namioka-type monochromator. The pulse duration of the SR light was about 1.6 ns. The second harmonic light of a Nd:YAG laser ($\hbar\omega_{laser}$ = 2.33 eV) was introduced in the opposite direction. The averaged power of the laser was about 10 W. The trigger signal for the laser was provided by the master oscillator of a RF cavity of the storage ring through a divider which lowered the frequency of the pulses down to about 5 kHz. The time interval between successive SR pulses was about 11 ns, while the duration of the laser pulse was about 800 ns.

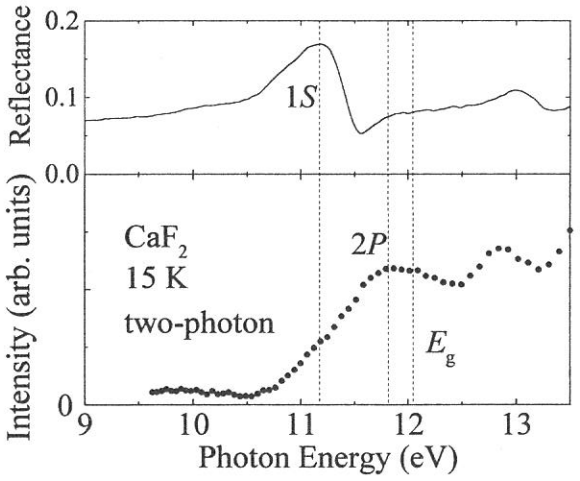


Fig. 2 Lower panel: TPS spectrum of $CaF_2$ at 15 K. Upper panel: Reflection spectrum.

We detected STE luminescence as the TPS signal by using a micro-channel plate photomultiplicr tube (MCP-PM) with narrow-band filters and a monochromator for eliminating the scattered light from the laser. The signal from the MCP-PM was fed to a three-channel time-gated photon counter. The photon signals just before and after the incidence of the laser pulses were counted at Channels 1 and 2, respectively: Channel 1 (CH1) counts the background signal induced only by the SR light, while CH2 counts the signal due to the simultaneous irradiation with SR and laser. The gate widths for both counters were set to be 4 $\mu$ s. CH3 counts the signal all the time for reference. The net luminescence signal induced by two-photon excitation was obtained by subtracting the count at CH1 from that at CH2. A few tens of seconds were required to accumulate the signal at a fixed wavelength. It is noteworthy that our experimental technique is a kind of zero method, and therefore it will be more sensitive than the transmission method that was applied to observe two-photon absorption of KI, KCl and NaCl by an Italian group [7].

Solid circles in the lower panel of Fig. 2 show the TPS spectrum of $CaF_2$ at 15 K. The abscissa of the figure represents the sum of photon energies of the SR and laser. The reflection spectrum is drawn by a solid line in the upper panel for comparison. The 1*S* peak at 11.2 eV in the reflection spectrum is indicated by an arrow. The TPS signal intensity rises at about 10.6 eV, and reaches a peak at 11.8 eV. We assign the peak to the TPS signal due to the 2*P* state of the $\Gamma$ exciton because of the parity-selection rule. The reflection spectrum also has a shoulder at that energy position. We assign the shoulder to the 2*S* state of the exciton on the basis of the observation of the 2*P* peak in the TPS spectrum.

Assuming the simple hydrogen-like energy levels or Wannier exciton picture, the *n*th level ($n$=1,2,3...) of the exciton, $E_n$, is given by

$$E_n = E_g - \frac{R^*}{n^2}, \qquad (1)$$

where $E_g$ is the band gap, and $R^*$ the exciton binding energy. By using eq. (1), we estimate the binding energy of the exciton in $CaF_2$ at 0.8 eV. It is about 0.2 eV smaller than that in Ref. 6. In the case of $BaF_2$ our value is 0.9 eV, and it is about 0.3 eV larger than that in Ref. 6. These previous values are based on band gap energies determined by analysis of reflection and one-photon absorption spectra. On the other hand, the present analysis based on clear peaks due to 2*P* excitons. This makes the present result more reliable than the previous values.

This work was partially supported by the Grant-in-Aid for Scientific Research from the Japanese Ministry of Education, Science, Sports and Culture.

References

[1] T. Tsujibayashi *el al.*: UVSOR Activity Report **24** (1997) 52.
[2] O. Arimoto *el al.*: UVSOR Activity Report **25** (1998) 116.
[3] S. Asaka *el al.*: Rev. Sci. Instrum. **69** (1998) 1931.
[4] M. Kamada *el al.*: J. Synchrotron Radiation **5** (1998) 1035.
[5] O. Arimoto *el al.*: J. Electron Spectrosc. Relat. Phenom. **92** (1998) 219.
[6] T. Tomiki and T. Miyata: J. Phys. Soc. Jpn. **27** (1969) 658.
[7] M. Casalboni *el al.*:Phys. Rev. B **44** (1991) 6504.

(BL1B)

# VUV excitation spectra of long persistent phosphorescence in $SrAl_2O_4$:Eu,Dy

M. Kamada, J. Murakami,[A] N. Kida,[B] N. Ohno,[B] T. Hasegawa,[C] J. Azuma,[C] and K. Tanaka[C]

*UVSOR Facility, Institute for Molecular Science, Myodaiji, Okazaki 444-8585*
*[A]Faculty of Engineering, Shinshu University, Nagano 380-8553*
*[B] Division of Elector. and Appl. Phys., Osaka Electro-Commun. Univ., Neyagawa 572-8530*
*[c] Faculty of Science, Kyoto University, Sakyo, Kyoto 606-8224*

In recent years, a new type of long persistent phosphors has been synthesized. The phosphors, for examples $SrAl_2O_4$:Eu, Dy and $CaAl_2O_4$:Eu,Nd, are much different from previous sulfide phosphors. The brightness and persistent time of the new phosphors are more than 10 times larger than the previous ones. Although the new long persistent phosphors attract much interest from application points of view, they are also very interesting materials for basic science. The carriers to provide the new long persistent phosphorescence are seemed to be holes, while those in the previous sulfide phosphors are electrons. The purpose of the present study is to know the long persistent phosphorescence induced by vuv excitation in order to investigate energy storage of vuv light.

The experiments were carried out at BL1B, where a 1-m Seya-Namioka type monochromator provides vuv light for excitation. Powders of pure and Eu-and Dy-doped $SrAl_2O_4$ were kindly supplied from Nemoto-Chem. Co. Ltd. The emission spectra were obtained by using a Princeton CCD system with a Spex 270M monochromator. The excitation spectra of $SrAl_2O_4$:Eu, Dy were measured in the range from 50 to 420 nm. The emission and excitation spectra of pure $SrAl_2O_4$ were also measured for comparison. Special cares were taken to separate long phosphorescence and short luminescence. After glow was also obtained with the vuv beam shutter being closed.

Figure 1 shows the emission spectra of $SrAl_2O_4$and $SrAl_2O_4$:Eu,Dy at 15 K under excitation by 180 nm. Strong emission bands are observed at about 450 and 520 nm in $SrAl_2O_4$:Eu,Dy. Weak bands are also appreciable around 250 and 360 nm. On the other hand, emission bands are observed around 250 and 360 nm in $SrAl_2O_4$. This indicates that the emission bands at about 450 and 520 nm are attributed to the impurity (Eu, Dy), while the bands around 250 and 360 nm are due to the host material ($SrAl_2O_4$).

Figure 2 shows excitation spectra of the emission bands mentioned above. The 450-nm and 520-nm emission bands in $SrAl_2O_4$:Eu,Dy are seen in the short-wavelength region below 400 nm. The 250-nm and 360-nm emission bands are observed in the wavelength region shorter than 190 nm. It should be noticed that the spectral profiles of the 450-nm and 520-nm emission bands in the wavelength region shorter than 190 nm are very similar with those for the 250-nm and 360-nm emission bands. This indicates that the 450-nm and 520-nm emission bands in $SrAl_2O_4$:Eu,Dy can be produced by energy transfer from host $SrAl_2O_4$. The mechanism of this host-sensitization is under consideration

The authors would like to express their sincere thanks to Mr. Y. Murayama of Nemoto Chem. Co.Ltd. for his kind supply of the present samples.

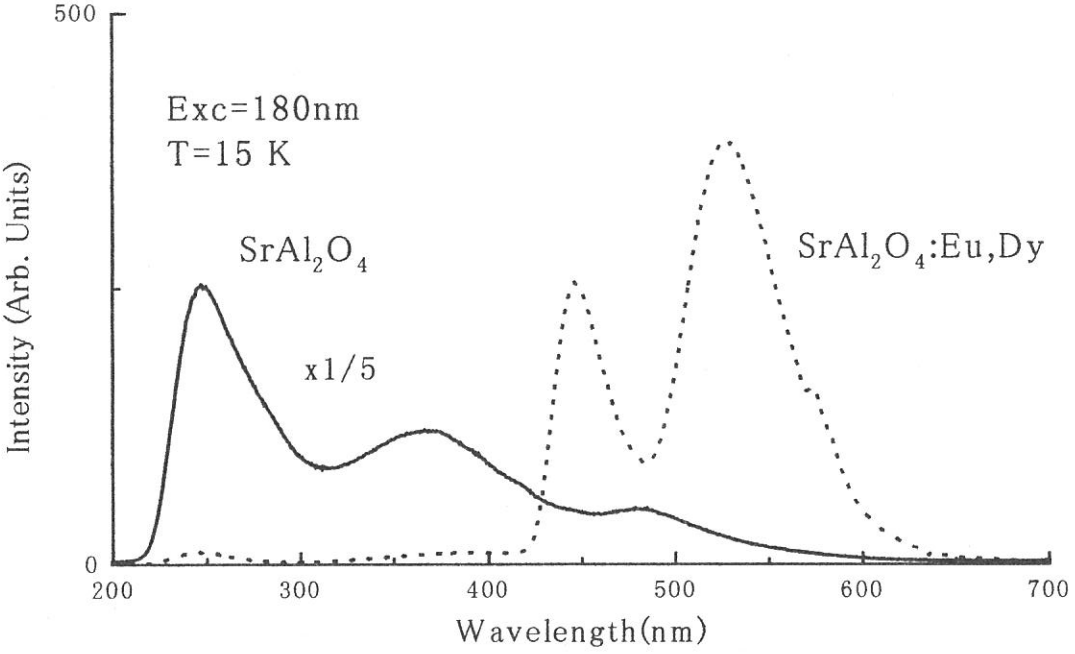


Fig. 1. Emission spectra of $SrAl_2O_4$ and $SrAl_2O_4$:Eu,Dy

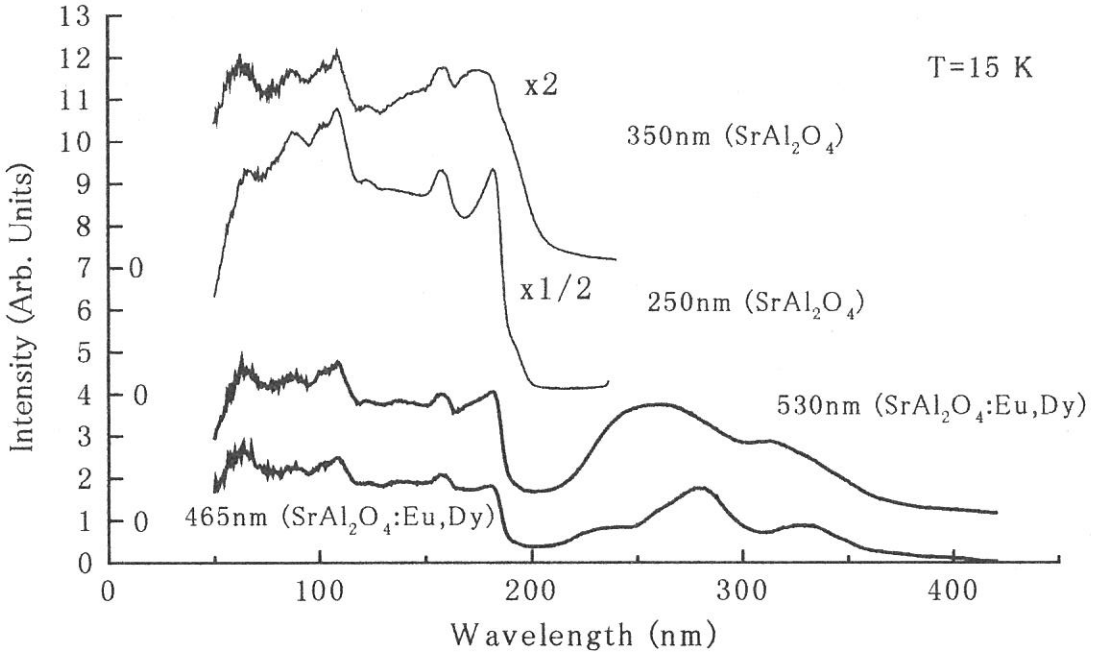


Fig. 2. Excitation spectra of $SrAl_2O_4$ and $SrAl_2O_4$:Eu,Dy

(BL1B)

# Formation Processes of Secondary Excitons and Electron-Hole Pairs by Vacuum Ultraviolet Radiation in $PbCl_2$ Crystal

M. Kitaura[1], M. Itoh[2], Y. Bokumoto[2] and M. Fujita[3]

[1]*Department of Physics and Mathematics, Fukui National College of Technology, Sabae 916-8507*

[2]*Department of Electrical and Electronics Engineering, Shinshu university, Nagano, 380-8553*

[3]*Maritime Safety Academy, Kure, 737-8512*

The use of synchrotron radiation (SR) allows us to obtain information on relaxation processes of elementary electronic excitations (EE's) in ionic crystals over a wide energy region. For example, Lushchik *et al.* have measured excitation spectra for intrinsic luminescence of alkali halides in a vacuum ultraviolet (vuv) region, and succeeded in discriminating several relaxation processes accompanied with multiplication of EE's (MEE's) [1]. We are interested in relaxation and migration of elementary EE's under conditions of MEE's in lead chloride ($PbCl_2$). The $PbCl_2$ crystal contrasts well with alkali halides with respect to the following points. First, the exciton absorption has features of the intra-ionic $6s^2 \rightarrow 6s6p$ transition in $Pb^{2+}$ ions [2]. Second, the intrinsic defect is described as a dimer $Pb_2^{3+}$ ion in which an electron is self-trapped at a pair of adjacent lead ions [3]. Third, the valence band is wider than the band gap and consists of lead $6s$ and chlorine $3p$ orbitals [4]. The aim of the present study is to investigate the interrelation between the electronic band structures and the relaxation of primarily created EE's in $PbCl_2$.

Optical properties of $PbCl_2$ have been studied extensively so far. In especial, luminescence studies have been carried out energetically because they give complementary information on the initial process of the photolysis in this material. Two types of luminescence are known to be observed in $PbCl_2$ [5,6]. The one is the UV luminescence produced under excitation in the lowest exciton band, which has been attributed to radiative decay of the self-trapped excitons at $Pb^{2+}$ ion sites. The other is the BG luminescence stimulated by photons with energies above the band gap, which originates from tunneling recombination of a hole released from some trapping center with an electron trapped at the $Pb_2^{3+}$ self-trapped electron (STEL) center. Formation processes of secondary excitons and *e-h* pairs by high energetic EE's will be, therefore, easily distinguished by measuring excitation spectra for the UV and BG luminescence in a vuv region.

In the present work, we have measured reflectance spectrum and excitation spectra for the UV and BG luminescence up to 30 eV. A similar measurement has been undertaken independently by Kink *et al* [7]. For the excitation spectra, reflection losses of an excitation light by the crystal surface were corrected by referring to the reflectance spectrum. The excitation spectra for the UV and BG luminescence, thus obtained, are shown in Fig. 1 (a) and (b), respectively. In spite of the correction for reflection losses by the surface, both the excitation spectra exhibit prominent dips at reflectance peaks in the energy region below 15 eV. The dips should be connected with nonradiative annihilation of EE's at the crystal surface, because optical excitation at the reflectance peaks with high absorption coefficient creates EE's at the crystal surface.

The UV luminescence yield $\eta_{UV}$ begins to increase sharply at 9.6 eV, similarly to the reflectance. Such an increase in $\eta_{UV}$ takes place around twice the value of the band gap energy, and thus originates from formation of secondary excitons by inelastic scattering of hot photoelectrons. The threshold energy for the secondary exciton formation $E_{th}^0 = 9.6$ eV exceeds the sum of the minimum energies required for creation of an exciton and of an *e-h* pair, namely, $E_{ex} + E_g = 9.2$ eV. The excess energy $E_{th}^0 - (E_{ex} + E_g) = 0.4$ eV would be gained by a valence hole created primarily. The condition $E_{th}^0 > E_{ex} + E_g$ has been satisfied in most of ionic crystals. We suppose that the spectral region of 9.6 - 20 eV, where $\eta_{UV}$ is relatively flat, is characterized by creation of a photohole in the valence band and a hot photoelectron in a higher conduction band. Our cluster calculation of $PbCl_2$ well explains the reflectance spectrum by considering the higher conduction band to be of the lead $6d$ orbital. The value of $\eta_{UV}$ does not almost change as the photon energy increases up to 30 eV. Therefore, it is most likely that, in the whole spectral range investigated here, the formation of secondary excitons arises from creation of hot photoelectrons in the lead $6d$ conduction band.

We observe a stepwise increase of the BG luminescence yield $\eta_{BG}$ around integral multiples of the band gap energy. The value of $\eta_{BG}$ is gradually enhanced in the range 14 - 20 eV, reaching almost twice as high as at 14 eV where one photon creates one *e-h* pair. These results undoubtedly satisfy conditions for multiplication of *e-h* pairs; therefore, excitation with photons of 14 - 20 eV leads to formation of secondary *e-h* pairs. Although

self-trapping of electrons is observed in $PbCl_2$, photoelectrons get high kinetic energy in the secondary *e-h* pair formation. The kinetic energy of the photoelectrons nearly equals to the excess energy $E_{th}^{\pm} - 2E_g = 4.4$ eV, which is gained by a photohole. On the basis of this result, we suppose that at low temperatures the $PbCl_2$ crystal exhibits both electron and hole self-trapping in the absence of an exciton effect. In the 17 - 20 eV range, we remark a slight increase in $\eta_{BG}$, which may arise from the electronic transition between the chlorine 3*s* outermost core band and the lead 6*p* conduction band. The value of $\eta_{BG}$ takes the minima at 21.4 eV, 22.7 eV, and 23.9 eV at which three peaks appear sharply in the reflectance spectrum. These reflectance peaks have been ascribed to creation of core excitons which consist of a hole in the lead 5*d* core states and an electron in the lead 6*p* conduction band. Such "cationic" core excitons will decay nonradiatively to produce an effective electron emission (i.e., Auger-decay process), resulting in the decrease of radiative recombination of a hole with the STEL center, i.e., the decrease of $\eta_{BG}$. This interpretation is based on the fact that the quantum yield of photoelectron emission in $PbCl_2$ has the maxima at the same energies as the reflectance peaks [8]. A further increase in the excitation photon energy brings about the treble value of $\eta_{BG}$ at 30 eV, that is, the energy at which one photon creates three *e-h* pairs. In this case, we expect that secondary valence excitations are generated through the following two processes. One is inelastic scattering of a hot photoelectron in the lead 6*p* conduction band, being described above. The other is nonradiative Auger-decay of a photohole in the chlorine 3*s* core band, which kicks up a valence electron into the high-lying conduction band.

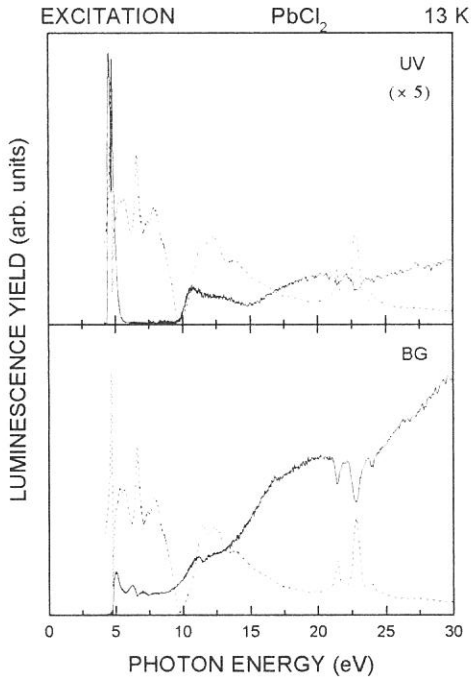


Fig. 1. Excitation spectra for the UV and the BG luminescence bands in $PbCl_2$ measured at 13 K The reflectance spectrum of $PbCl_2$ at 13 K is also shown by a broken curve for reference.

## References


[1] A.Lushchik, E.Feldbach, Ch.Lushchik, M.Kirm, and I.Martinson: Phys. Rev. B **50**, (1994) 6500.

[2]M.Fujita, H.Nakagawa, K.Fukui, H.Matsumoto, T.Miyanaga, and M.Watanabe:
J. Phys. Soc. Jpn., **60** (1991) 4393.

[3] S.V.Nistor, E.Goovearts, and D.Schoemaker: Phys. Rev. B **48**, (1993) 9575.

[4] M.Itoh, T.Shiokawa, K.Sawada, and M.Kamada: J. Phys. Soc. Jpn., **67** (1998) 2140.

[5] M.Kitaura and H. Nakagawa: J. Electron Spectrosc. and Relat. Phenom., **79** (1996) 171.

[6] M.Kitaura and H. Nakagawa: J. Lumi. **72-74** (1997) 883.

[7] R.Kink, T. Avarmaa, V.Kisand, A.Lohmust, I.Kink, and I.Martinson:
J. Phys.: Condense. Matter **10** (1998) 693.

[8] M.Itoh: J. Fac. Eng. Shinshu University, (1998) 19.

(BL-1B)

# Vacuum Ultraviolet Absorption Spectra of Amino Acids

M. Tanaka, Y. Kishigami, I. Shimoyama[1)], K. Ebina[2)] and K.Nakagawa[2)]

Graduate school of Cultural Studies and Human Science, Kobe University, Tsurukabuto, Nada-Ku, Kobe 657-8501

[1)]Graduate school of Science and Technology, Kobe University, Rokkohdai, Nada-Ku, Kobe 657-8501

[2)]Faculty of Human Development, Kobe University, Tsurukabuto, Nada-Ku, Kobe 657-8501

Vacuum ultraviolet absorption spectra of aspartic acid (Asp) and phenylalanine (Phe) were measured in the region of 40 nm to 250 nm.

Evaporated thin films of Asp and Phe was carefully prepared with a new technique developed by our group, in which amino acids were evaporated on the sodium salycilate (SS) films. Thickness $d$ of the films were 42 nm for Asp and 33 nm for Phe. Measurements of spectra were performed at the beamline BL-1B at room temperature. Measuring the fluorescence intensity of SS without amino acids as the reference spectra $I_0(\lambda)$ and that with amino acids as $I(\lambda)$, absorption coefficient $\mu(\lambda)$ were calculated from the Lambert-Beer's law $I(\lambda) = I_0(\lambda)\exp(\mu(\lambda)d)$.

Absorption spectral shape obtained for Asp was in a good agreement with that reported by Nakagawa et al.[1], in which spectrum was measured in the region of 140 nm to 250 nm. But absolute values of $\mu(\lambda)$ obtained in this work were smaller than that by Nakagawa et al.[1] by a factor of 2.1 in the region of 140 nm to 250 nm. We assumed that the thickness of our films on the SS was not uniform because substrates of our experiment were non-flat SS, and we multiplied a factor of 2.1 to the $\mu(\lambda)$ obtained in this work. The curve A in Fig. 1 shows the absorption spectrum of Asp after this correction at $\lambda$ =147 nm.

With a similar procedure we obtained absorption spectra of Phe. In the case of Phe, since the strong fluorescence was observed around 190 nm, we connected our spectrum with that by Nakagawa et al.[1] at $\lambda$ =147 nm. The curve B in Fig. 1 shows the absorption spectrum of Phe after this correction. Curve B' in the figure is the spectra reported by Nakagawa et al.[1].

Assignment of peaks in these spectra are of great interest and we have a plan to make a quantum mechanical calculation of energy levels of these amino acids together with some theorists.

Reference

[1]K. Nakagawa et al., in "The Role of Radiation in the Origin and Evolution of Life", ed. by M. Akaboshi et al., Kyoto University Press (1999), Kyoto Japan, in press.

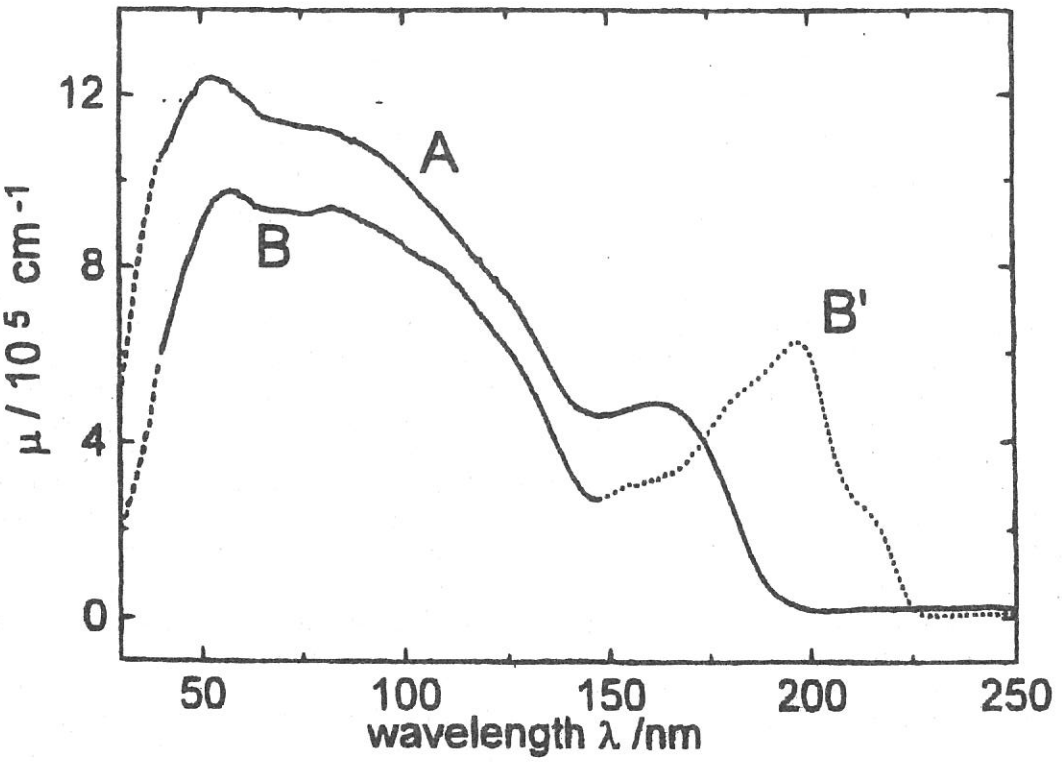


Fig. 1. Absorption spectra of aspartic acid (Curve A) and Phenylalanine (Curve B and B').

(BL1B)

# Self-Trapped Exciton Luminescence in $BaF_2$ Stimulated under Simultaneous Irradiation of Synchrotron Radiation and Laser

M. Watanabe, M. Iwanaga[a], S. Asaka[b], T. Tsujibayashi[c], O. Arimoto[d], M. Itoh[e], S. Nakanishi[f], H. Itoh[f] and M. Kamada[g]

*Department of Fundamental Sciences, Kyoto University, Kyoto 606-8501*

[a]*Graduate School of Human and Environmental Studies, Kyoto University, Kyoto 606-8501*

[b]*Equipment Development Center, Institute for Molecular Science, Okazaki 444-8585*

[c]*Department of Physics, Osaka Dental University, Hirakata 573-1121*

[d]*Department of Physics, Okayama University, Okayama 700-8530*

[e]*Department of Electrical & Electronic Engineering, Shinshu University, Nagano 380-8553*

[f]*Department of Advanced Materials Science, Kagawa University, Takamatsu 760-8526*

[g]*UVSOR Facility, Institute for Molecular Science, Okazaki 444-8585*

$BaF_2$ is a widely-used material as a scintillator in many fields such as high-energy physics and nuclear medicine. Therefore, its fundamental information about radiation damages due to defect formation is important for practical uses. Recently we have developed a spectroscopic system utilizing synchrotron radiation (SR) and laser as light sources, and applied it to two-photon spectroscopy of BaF2 [1]. In the present work we apply our system to photostimulated-luminescence method which is a very sensitive tool to detect radiation damages generated in samples. We report that photostimulation occurs for self-trapped exciton (STE) luminescence under simultaneous irradiation of SR and laser. The present result indicates that lattice defects are generated in $BaF_2$ even under the irradiation with relatively weak light beam compared to $\gamma$-ray or neutron.

Single crystal of $BaF_2$ obtained from the Horiba Ltd. was used here. Experiments were performed with a combination of the SR and a cw mode-locked Ti:sapphire laser (wavelength 780 nm, pulse width 100 fs, repetition rate 90 MHz, average power 500 mW). In our experiments, both the SR and the laser were used as cw light sources. The sample with a cleaved (111) surface was mounted on a copper finger of a temperature-variable cryostat. The SR beam, dispersed by a 1m Seya-Namioka type monochromator, irradiated the sample surface under normal incidence configuration, and the laser beam was incident from an opposite direction of the SR beam. Luminescence was detected through a monochromator equipped with a photomultiplier.

Figure 1 shows luminescence spectra under the SR excitation (○), and the simultaneous irradiation of the SR and the laser (●). The sample was irradiated with the SR at 19.5 eV, which corresponds to the transition from the $Ba^{2+}$ 5p core band to the conduction band [2]. Two emission bands centered at 5.5 eV and 4.1 eV are assigned to the Auger-Free and the STE luminescence, respectively [3]. One can see that emission intensity increases by the simultaneous irradiation. Difference between the two spectra, i.e., net signal intensity induced by the simultaneous irradiation is shown by closed squares. It is evident that the laser irradiation stimulates only the STE luminescence. The signal intensity was found to increase linearly with the laser power.

Figure 2 shows the dependence of the signal intensity induced by the simultaneous irradiation on the SR photon energy. As the photon energy is increased from the valence excitation at around 10 eV, the signal intensity begins to increase and becomes remarkable in a region from 16 to 21 eV, followed by the decrease in the higher energy region. The energy region from 16 to 21 eV is mainly characterized by several core-exciton transitions [2]. It is suggested that the photostimulation effect observed by us is related to the formation of core excitons.

In order to investigate the mechanism of the photostimulation effect, we measured the stimulated signal intensity as a function of temperature. The result is presented in Fig.3. The

signal intensity gradually increases with increasing temperature, but abruptly decreases above 100 K. Beaumont *et al* reported that, in $BaF_2$, a $V_K$ center (self-trapped hole) is thermally released above 100 K [4]. Then it is reasonable to consider that the photostimulation effect is ascribed to the generation of $V_K$ centers.

In alkali halides, it is well known that photostimulation of the STE luminescence occurs under simultaneous irradiation of UV and red light [5]. The photostimulated STE luminescence arises from the recombination of a $V_K$ center and an electron released from some trapped center by the red light. Since formation process of the STE luminescence in $BaF_2$ is quite similar to that in alkali halides, we conclude that the photostimulation effect in $BaF_2$ is due to the capture of an optically released electron by the $V_K$ center. We also measured the time response of the photostimulated signal, when the laser beam was periodically turned on and off during steady irradiation of the SR. Whenever the laser beam was turned on, the signal rose instantaneously in our time resolution, and decayed with a time constant of a few ms to a stationary value. The peak height of this short-lived spike was found to increase with the period of the SR irradiation. This fact indicates that the steady irradiation of the SR continues to generate trapping centers of electrons and holes. That is, lattice defects are generated even under the irradiation of weak light beam such as the SR. The experimental result in Fig.2 may suggest that the dissociation of core exciton is effective for defect formation in $BaF_2$. Further studies are in progress.

This work is supported by a Grant-in Aid for Scientific Research from The Ministry of Education, Science, Sports and Culture of Japan.

**References**

[1] O. Arimoto *et al* : J. Electron Spectroscopy and Related Phenomena **92** (1998) 219.
S. Asaka *et al* : Rev. Sci. Instrum. **69** (1998) 1931.
[2] G. W. Rubloff : Phys. Rev. B**5** (1972) 662.
[3] M. Itoh *et al* : Rev. Solid State Sci. **4** (1990) 467.
[4] J. H. Beaumont *et al* : Proc. R. Soc. London A **315** (1970) 69.
[5] M. Itoh : J. Phys. Soc. Jpn. **53** (1984) 1191.

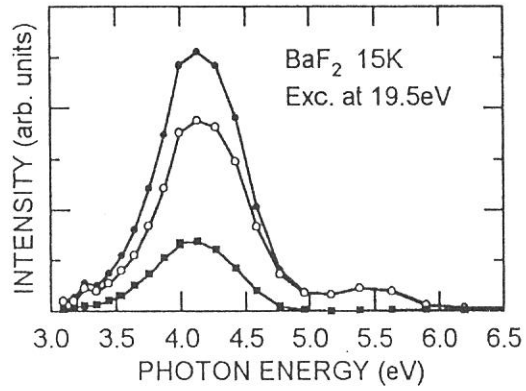


Fig.1 Luminescence spectra of $BaF_2$ under the excitation with SR (○), and the simultaneous irradiation with SR and laser (●). Difference between the two spectra is also shown by closed squares.

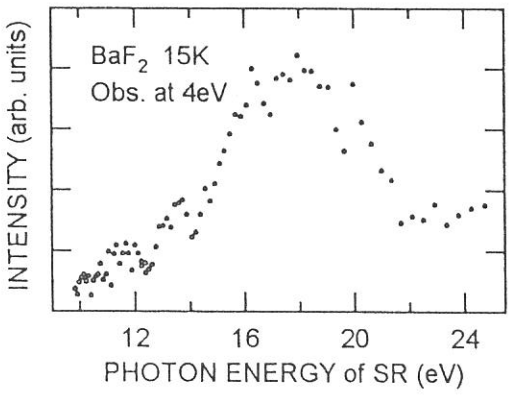


Fig.2 Dependence of the photostimulated signal on the photon energy of SR.

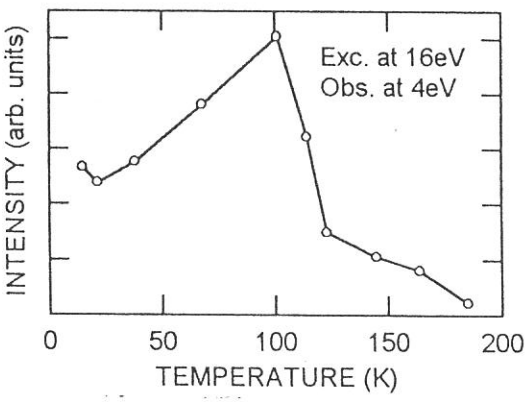


Fig.3 Temperature dependence of the photostimulated signal intensity.

# (BL1B) One-Photon Photoionization Thresholds of Aromatic Molecules at Water/Air Surface

Teiichiro Ogawa[A], Shinya Sasaki, Manabu Tokeshi[B], Takanori Inoue[C], and Akira Harata[A]

*Department of Molecular Science and Technology, Kyushu University*
*Kasuga-shi, Fukuoka, 816-8580*

Photoionization behavior at the solution surface is different from that in the bulk solution. Photoionization threshold in solution has been determined in a single-photon process using synchrotron radiation or hydrogen discharge lamp, and in a two-photon process using laser radiation. Although there are a few measurements on photoionization threshold of aromatic molecules on solution surface using laser two-photon excitation, no measurements have been carried out using one-photon excitation on solution surface. We have tried to measure one-photon ionization spectra (energy dependence of photoionization efficiency) and photoionization thresholds of aromatic molecules on water surface using synchrotron radiation.

The experimental apparatus is shown in Fig. 1. Synchrotron radiation of energy from 4.7 to 7.5 eV was used as an excitation source. The beam power was monitored using a photomultiplier to calibrate its energy dependence. It was about $10^{10}$ photon/s at 6.2 eV, and varied as shown in Fig. 2. The beam was softly focused through a sapphire lens and irradiated the solution surface at 85° to the surface normal. The solution was kept in a stainless-steel vessel (0.1 mL) of 8 mm in diameter, and the vessel was served as the current collecting electrode. A disk electrode was located 5 mm above the solution surface and was connected to a high-voltage power supply unit. The photoionization current was measured using a current meter (Keithley, 617). The perylene (guaranteed grade, Nacalai Tesque) was used as recieved. The water was distilled, deionized, filtered and distill again in a quartz vessel.

The one-photon ionization spectra of perylene on the water surface have been measured and its intensity was linearly proportional to its concentration for $10^{-6}$ - $10^{-8}$ M. The photoionization spectrum was nomalized by beam power and solution concentration. The blank signal (signal of pure water) was relatively small and was not dependent of the excitation energy.

The photoionization current near threshold can be represent by a power law,

$$I = c(E_{excess})^{5/2} = c(h\nu - I_{th})^{5/2}$$

where $E_{excess}$ is the excess energy of the ionized pair, $h\nu$ is the photon energy and $I_{th}$ is the ionization threshold. A plot of the (2/5)th power of the normalized photoionization current versus the photon energy should give a straight line, and its onset on the abscissa should give $I_{th}$, because there would be no photoionization current below $I_{th}$. Figure 3 shows the photoionization spectra of perylene molecules on water surface, and $I_{th}$ of perylene has been determined to be 5.9 eV. $I_{th}$ of perylene was determined to be 5.95 eV by a two-photon process using a Ti-sapphire laser and agree with the present value within experimental errors.

The photoionization threshold on the surface has been related with the ionization potential in gas phase, $I_p$, as:

$$I_{th} = I_p + P^+$$

where $P^+$ is the polarization energy of the positive ion. This equation should be applicable to these molecules in this study, because the electron escapes directly from the surface and so the electron affinity of the solvent is able to be negligible. $P^+$ of perylene on water can be determined as -0.9 eV. The value of $P^+$ can be obtained from Born equation using the dielectric constant and the radius of the molecule. The observed value of $P^+$ was about half as much as the calculated value, this indicates that the effective dielectric constant of water surface should be much smaller than that of bulk water, 80.4 at 20°C.

[A] Present address: Department of Molecular and Material Sciences , Kyushu University, Kasuga-shi, Fukuoka, 816-8580
[B] Present address: Integrated Chemistry Project, Kanagawa Academy of Science and Technology, Kawasaki-shi, Kanagawa, 213-0012
[C] Present address: Department of Applied Chemistry, Ohita University, Dannoharu, Ohita, 870-1124

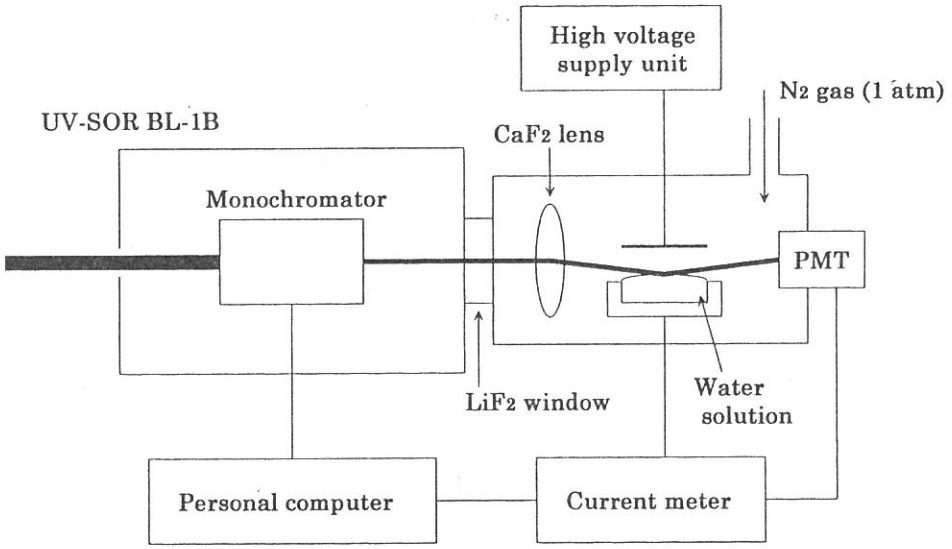


Fig.1 Schematic diagram of the experimental apparatus.

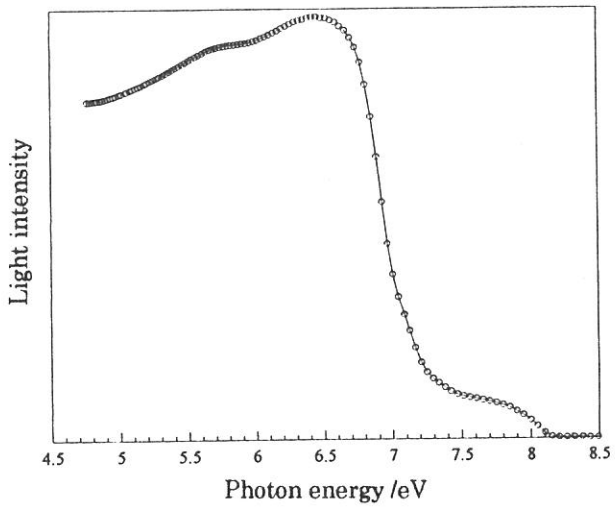


Fig.2 The intensity of the excitation light.

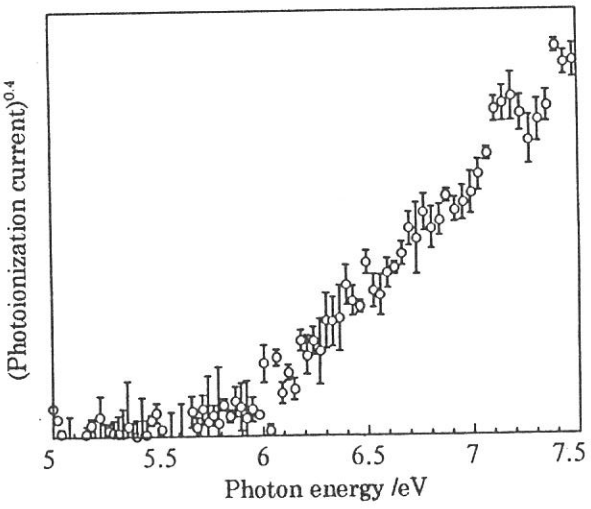


Fig.3 Photoionization spectra of perylene.

Reference
1. Inoue, T.: Sasaki, S.: Tokeshi, M.: Ogawa, T., *Chem. Lett.*, 1998, 609
2. Holroyd, R. A.: Preses, J.M.: Zevos, N., *J. Chem. Phys.*, 79 (1983) 483.
3. Ogawa, T.: Chen, H-T.: Inoue, T.: Nakashima, K., *Chem. Phys. Lett.*, 229 (1994) 328.
4. Watanabe, I.: Ono, K.: Ikeda, S., *Bull. Chem. Soc. Jpn.*, 64 (1991) 352.
5. Born, M., *Z. Physik*, 1 (1920) 45

(BL1B)

# Optical Spectra of $PbF_2$ Crystals in the VUV Region

Masami FUJITA, Minoru ITOH[A], Jun-ichi MURAKAMI[A], Yoshitoshi BOKUMOTO[A]
Mamoru KITAURA[B], Hideyuki NAKAGAWA[C] and Dmitri L. ALOV[D]

*Maritime Safety Academy, Wakaba, Kure 737-8512*
[A]*Department of Electrical and Electronic Engineering, Faculty of Engineering, Shinshu University, Wakasato, Nagano 380-8553*
[B]*Fukui National College of Technology, Geshi, Sabae 916-8507*
[C]*Department of Electrical and Electronics Engineering, Faculty of Engineering, Fukui University, Bunkyo, Fukui 910-8507*
[D]*Institute of Solid State Physics, Chernogolovka, Moscow 142432 Russia*

Lead fluoride is an interesting material because it has two structural modifications which coexist at normal conditions. The orthorhombic phase ($\alpha$-$PbF_2$) is more stable below 320℃, but the cubic phase ($\beta$-$PbF_2$) is also metastable at low temperatures. Optical spectra of $\beta$-$PbF_2$ have been measured previously using polished surface and evaporated film[1], because flat surface cannot be obtained by the cleavage of the cubic crystal. It is known that the phase transition of $\beta$-$PbF_2$ into $\alpha$ phase is caused by application of pressure. In the present experiment, reflection spectra have been measured in order to examine the effect of surface treatment on the optical spectra and to investigate the electronic structure in lead fluoride.

Single crystals of $\alpha$-$PbF_2$ were grown from aqueous solution. Reflection spectra were measured using the as-grown surface which contains the *ab*-plane. Single crystals grown by the Bridgman method were used for the measurement of $\beta$-$PbF_2$. Experiments were performed at BL1B of UVSOR.

Reflection spectra of $\alpha$-$PbF_2$ crystal at LHeT are shown in Fig. 1(a) for $E//a$ and $E//b$ polarization. Figures 1(b) and 1(c) show the reflection spectra of $\beta$-$PbF_2$ for a polished surface and for a cleaved surface, respectively. The peak at 5.7 eV in each spectrum is due to the lowest exciton transition. The exciton band in Fig. 1(a) exhibits dichroism and the exciton band in Fig. 1(c) has three fine structures[2]. It was found that the spectral shape of the exciton band in Fig. 1(b) can be fitted well by the average of the spectra for $E//a$ and $E//b$ in Fig. 1(a). The spectrum in the 6-7 eV region in Fig. 1(b) exhibits intermediate features between Fig. 1(a) and (c). These facts indicate that the phase transition on the surface of cubic crystal into orthorhombic phase is induced by the stress during mechanical polishing. We regard the spectrum of the cleaved surface as intrinsic to $\beta$-$PbF_2$.

Figure 2 shows reflection spectra of $\alpha$- and $\beta$-$PbF_2$ up to 30eV. In the 10-13 eV region, several sharp peaks are observed in $\beta$-$PbF_2$. They are attributed to the transitions from both $F^-$ $2p$ valence band and $Pb^{2+}$ $6s$ valence band. The structures in the 14-19 eV region are due to the transition from the valence band to the $Pb^{2+}$ $6d$ conduction band, according to our cluster

calculation. On the other hand, broad structures are observed in $\alpha$-$PbF_2$ in 10-19 eV region. The cluster calculation shows that the $F^-$ $2p$ valence band of $\alpha$-$PbF_2$ is rather wide and complicated compared to $\beta$-$PbF_2$, because of the lower symmetry of the crystal structure. The difference in the valence band structure would be reflected in the optical spectra in 10-19 eV region.

Sharp peaks observed in the 20-25eV region are due to the exciton transition from $Pb^{2+}$ $5d$ core level to the $6p$ level. The peaks 1, 2 and 3 are assigned to the transitions from $^1S_0$ ground state to the $J=1$ excited states of $^3P_1$, $^1P_1$ and $^3D_1$, as is the case of $PbCl_2$ and $PbBr_2$[3]. In addition to these main peaks, a small peak 0 is observed in both crystals and a peak 3' is observed in $\beta$-$PbF_2$. Some of the $J \neq 1$ excited states, which are optically forbidden in a free-ion state, can couple with the $J=1$ states through the crystal-field potential in each crystal. The additional peaks 0 and 3' are probably due to the transitions to such excited states. The appearance of these peaks in $\beta$-$PbF_2$ indicates that the crystal-field interaction in $Pb^{2+}$ $5d$ core level plays an important role as is the case of $Tl^+$ $5d$ core exciton in thallous halides[4], because the cubic crystal-field does not lift the degeneracy of $6p$ orbitals.

## References


[1]J. H. Beaumont, A. J. Bourdillon and J. Bordas: J. Phys. C Solid State Phys. **10**(1977)761.

[2]M. Fujita, M. Itoh, H. Nakagawa, M. Kitaura and D. L. Alov: J. Phys. Soc. Jpn. **67**(1998)3320.

[3]M. Fujita, H. Nakagawa, K. Fukui, H. Matsumoto, T. Miyanaga and M. Watanabe: J. Phys. Soc. Jpn. **60**(1991)4393.

[4]M. Fujita, N. Ohno, Y. Kiyama and K. Nakamura: J. Electron Spectrosc. Relat. Phenom. **79**(1996)59.


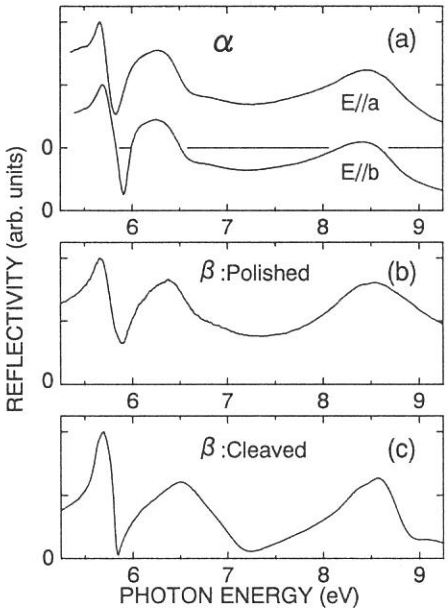


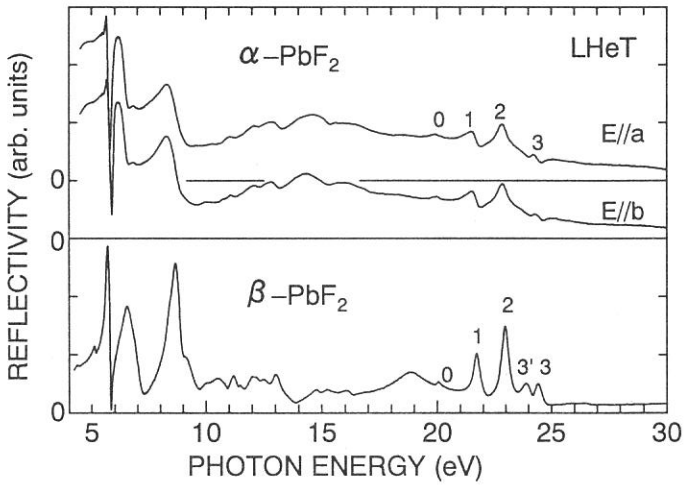


Fig. 2. Reflection spectra of $\alpha$- and $\beta$-$PbF_2$ crystals in the 5-30 eV region at LHeT.

Fig. 1. Reflection spectra of (a) $\alpha$-$PbF_2$, (b) $\beta$-$PbF_2$ for polished surface, and (c) $\beta$-$PbF_2$ for cleaved surface at LHeT.

(BL-1B)

# Photoluminescence from Quasi One Dimensional Crystal Piperidinium Tribromoplumbate

Junpei Azuma, Koichiro Tanaka and Ken-ichi Kan'no
*Department of Physics, Kyoto University*
Sakyo, Kyoto 606-8205, Japan

Piperidinium trihaloplumbate $C_5H_{10}NH_2PbX_3$ [X=I,Br] (abbreviated as PLX hereafter) is well known to have a self-organized 1D structure; two consecutive lead ions are bridged by three halogen ions to form polymeric chains. In other words, $[PbX_6]^{4-}$ octahedra connect to each other by sharing their faces. The piperidine cations, which connect two adjacent columns, isolate these polymeric chains.[1,2] These materials are suitable for the study of nano-scale quantum wires, which are difficult to synthesize in semiconductors by artificial methods.[3,4]

$C_5H_{10}NH_2PbBr_3$ (PLB) complex is synthesized from piperidine hydrobromide $C_5H_{10}NH_2Br$ and lead bromide $PbBr_2$ in dimethylformamide. Transparent and colorless single crystals were grown for 2-3 weeks by evaporating the solvent slowly at room temperature. Typical sizes of crystals are $1.0x1.0x7.0mm^3$.

Reflectivity and luminescence excitation measurements were performed at beam line BL-1B of UVSOR. The absolute value of reflectivity was determined by using reflectivity in the transparent region measured by a He-Ne laser.

Figure 1 shows polarized reflection spectra of PLB at 15K. There is strong anisotropy that the reflectivity for E//b polarization is several times as large as that for E⊥b polarization. This indicates that electrons and holes are confined within the polymeric chains. A peak with large oscillator strength appears at 3.9eV only for the light polarized parallel to the chains, which is assigned to the lowest exciton transition. The piperidine cations filling between chains are supposed to act as the barrier against the 3.9eV exciton, because the intramolculer absorption edge of the piperidine vapor is known to be located at 4.8eV. The lowest exciton peak of PLI is located at 3.3eV.[3] The band gap energy increases by 0.6eV through substitution of bromine ions for iodine ions of PLI.

It is well known that in alkali halide the highest occupied state of $Pb^{2+}$ impurity is the 6s orbital and those of halogen ions are np orbitals (Br: n=4, I: n=5).[5] These orbitals are mixed to form molecular orbitals, in which antibonding state is considered as HOMO of $[PbX_6]^{4-}$ octahedra. The lowest unoccupied state of lead ion is the 6p orbital and those of halogen ions are (n+1)s orbitals. LUMO of $[PbX_6]^{4-}$ octahedra should be the lead 6p orbital because the energy of (n+1)s orbitals are much higher than that of the lead 6p orbital. The substitution of bromine ions for iodine ions, therefore, makes the energy of HOMO decrease, resulting in the increase of the band gap energy.

The effect of substitution of bromine ions for iodine ions of PLI is almost the same as that of the $[PbX_6]^{4-}$ system in alkali halide, so that np orbiatls of halogen ions must be mixed strongly in the valence band of PLX system. (See inset in Fig. 1.)

Figure 2(a) shows a luminescence spectrum at 15K under 3.9eV excitation. Two emission bands appear at 3.0eV and 1.8eV, which are denoted as V emission and R emission respectively. Their large Stokes-shifts indicate strong exciton-lattice interaction in the excited states. A contour map of the emission efficiency at 15K is shown in Fig. 2(b), which is obtained by summarizing the luminescence spectra under various excitation energies. V and R emission can be stimulated above 3.8eV. Above 4.2eV the peak energy of R emission spectra shifts for the higher energy side around 1.85eV. It suggests that R emission band must be a composite emission band. In the low energy region below 3.8eV two luminescence bands are observed instead of V and R emission. These bands located around 2.6 and 1.9eV have extrinsic natures because they strongly depend on the sample preparation. Figure 2(c) shows excitation spectra for emission intensities at 3.0eV and 1.9eV. Above 4.2eV R emission is stimulated more

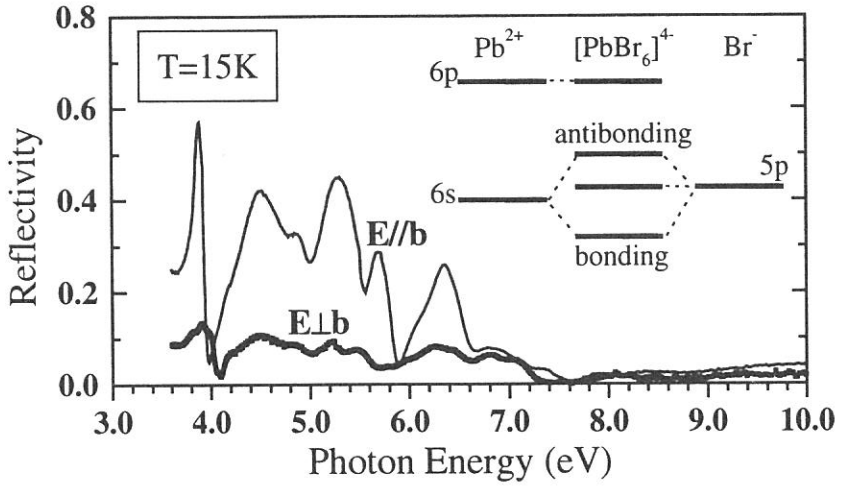


FIG. 1: Polarized reflection spectra of $C_5H_{10}NH_2PbBr_3$ at 15K. The indexes on the spectra show the polarization of the incident light. Inset shows schematic energy level diagram of $[PbBr_6]^{4-}$ octahedra.

**(BL-1B)**

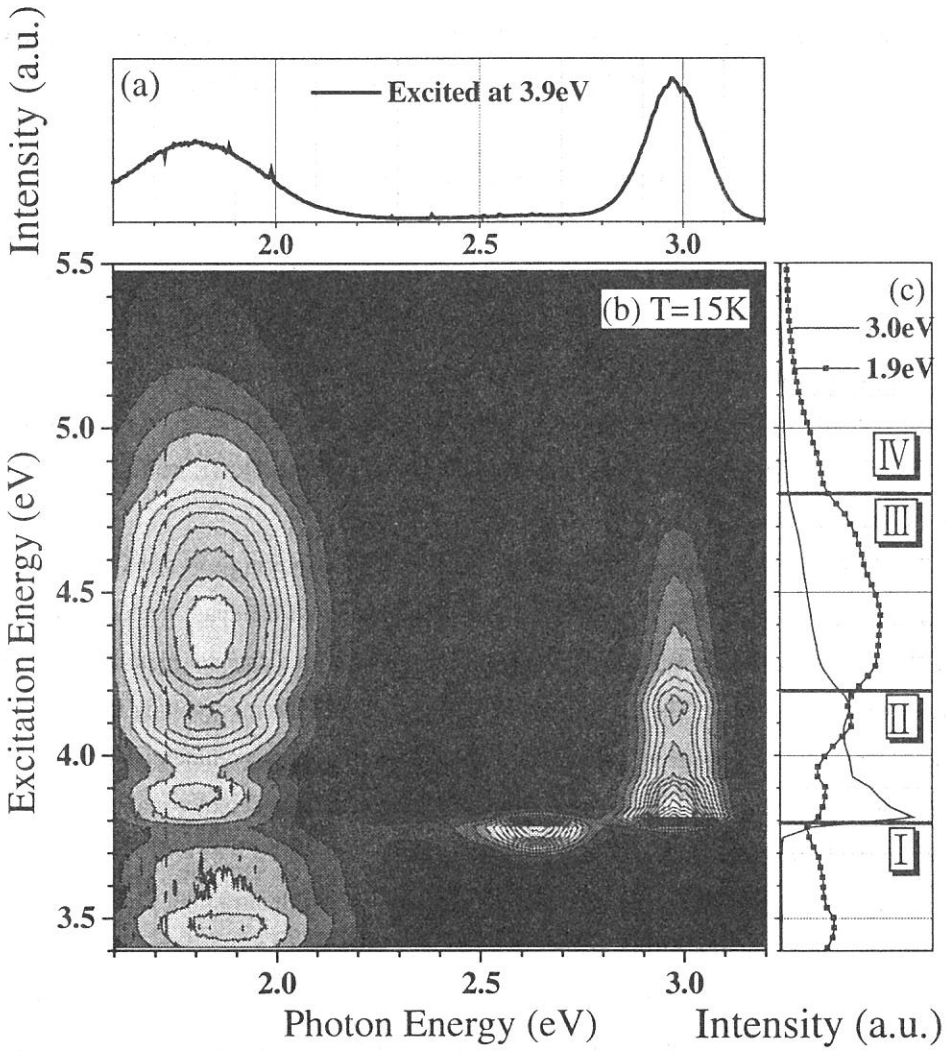


FIG. 2(a): Luminescence spectrum of $C_5H_{10}NH_2PbBr_3$ at 15K under 3.9eV excitation. Excitation light is polarized parallel to the b-axis. (b): Contour map representation of luminescence spectra under various excitation energies. (c): Excitation spectra detected at 3.0 and 1.9eV. This figure shows vertical cross sections of the contour map at 3.0 and 1.9eV. Four qualitative excitation regions are indicated. (See text.)

efficiently than V emission while below 4.2eV the R emission intensity is weaker than the V emission intensity. The excitation energy region higher than 4.8eV all emission efficiency becomes lower. Four distinct regions, therefore, can be recognized as Ⅰ to Ⅳ in Fig. 2(c).

In conclusion, several emission bands were found under excitation in the intrinsic absorption region. It suggests that multi-stability exists in the photo-excited state of PLB.

**References**

1. G. V. Gridnova, E. A. Ziger, V. M. Koshkin, S. V. Lindeman, Yu. T. Struchkov and V. E. Shklover, Doklady Akademii Nauk, 278, 414 (1984).

2. A. B. Corradi, S. Bruni, F. Cariati, A. M.Ferrari, A. Saccani, F. Sandrolini and P. Sgarabotto, Inorg. Chim. Acta., 254, 137 (1997).

3. A. Nagami, K. Okamura and T. Ishihara, Physica B, 227, 346 (1996).

4. G. C. Papavassiliou and I. B. Koutselas, Synth. Metals, 71, 1713 (1995).

5. T. Tsuboi, Phys. Status Solidi B, 96, 321 (1979).

(BL1B)

# Improvement of resolution of the detector for inverse photoemission spectrometer by coating KCl thin film on bandpass detector

Hiroshi YANAGI, Kazushige UEDA, Sakyo HIROSE, Syuntaro IBUKI, Tomomi HASE, Hideo HOSONO and Hiroshi KAWAZOE

*Materials and Structures Laboratory, Tokyo Institute of Technology, Yokohama 226-8503*

Inverse photoemission spectroscopy (IPES) is the most convenient technique to probe unoccupied electronic states of solids. Electron energy loss spectroscopy (EELS) and X-ray absorption spectroscopy (XAS), which also observe unoccupied states, give the partial density of states (PDOS), while IPES generally gives the total density of states (DOS).

IPES, which observes photons emitted from a sample by capturing electrons with a specified kinetic energy, has two different types; one detects isochromatic photons with bandpass detector and the other detects photons that have a variety of energies through a monochrometer with a channel plate amplifier and a position-sensitive resistive anode detector. The former type of IPES called BIS (bremsstrahlung isochromat spectroscopy) includes the Geiger-Müller counter with a $CaF_2$ entrance window or a commercial photomultiplier with an entrance window as a bandpass detector. The Geiger-Müller counter type detector realizes a resolution of 0.6eV as a full width at half maximum (FWHM) centered at the photon energy of 9.8eV. However, the photomultiplier type has advantages in high stability, no dead time and compatibility with ultra high vacuum. Ueda et al. reported that the sensitivity and resolution of the photon detector were improved by coating a KCl film of over 100nm thickness on the Cu-BeO first dynode [1]; the FWHM of 0.47eV centered at the photon energy of 9.8eV. In this article, we describe the results of application of this technique for improvement of resolution in our instrument.

The detector of photons installed in our BIS instrument is a commercial photomultiplier (Hamamatsu Photonics: R595) with a $SrF_2$ entrance window, which is a bandpass photon detector with FWHM of 0.75eV centered at 9.39eV. The constitution is as almost the same as the instrument used by Ueda et al. except that their first dynode of photomultiplier was coated with a KCl film. All components are mounted in ultra high vacuum chamber under the base pressure below $4\times10^{-8}$Pa.

The KCl film of 210nm was evaporated onto the Cu-BeO first dynode (Hamamatsu Photonics: E5055) of the photomultiplier under a vacuum of $7\times10^{-4}$Pa. The thickness of the film was evaluated by a quartz thickness monitor. The estimation of bandpass characteristics of the new bandpass photon detector was carried out on BL1B of UVSOR in Institute for Molecular Science.

Figure 1 shows the characteristics of the bandpass photon detector before and after the deposition of KCl film on the first dynode: the dashed and dotted curves are characteristics obtained before the deposition and the solid curve is that after deposition. Peak heights of the dotted curve and the solid curve are adjusted to each other for comparison of FWHM. The FWHM is reduced from 0.75 to 0.45eV by the deposition of the KCl film on the Cu-BeO first dynode. Furthermore, the intensity of the peak top of the solid curve is about 34 times as high as that of the dashed curve. The sensitivity was increased by about one order on the deposition of KCl thin film on Cu-BeO first dynode. Consequently, the improvement of the bandpass photon detector for our instrument was

successful.

**Reference**

[1] Y. Ueda, K. Nishihara, K. Mimura, Y. Hari, M. Taniguchi and M. Fujisawa, Nucl. Instrum. and Methods in Phys. Research, **A330**, 140(1993)

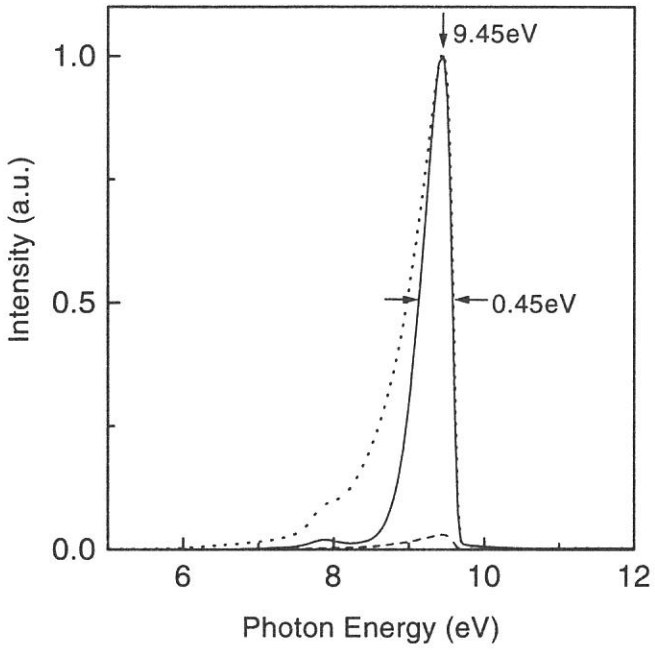


Fig. 1 Characteristics curves of bandpass detectors without (a dotted curve and a dashed curve) and with the KCl film (a solid curve) on the Cu-BeO first dynode of the photomultiplier. Peak heights of dotted curve and solid curve are adjusted to each other for comparison of FWHM.

(BL1B)

# VUV excitation spectra of a trace of impurities in $CaF_2$ single crystals for ArF excimer laser lithography

M. Mizuguchi, T. Ogawa, H. Yanagi and H. Hosono

*Materials and Structures Laboratory, Tokyo Institute of Technology, 4259 Nagatsuta, Midori-ku, Yokohama 226-8503, Japan*

## INTRODUCTION

Calcium fluoride single crystals are now attracting much interested as a lens material for ArF excimer laser (emission wavelength = 193 nm) lithography because of a large band gap of ~12 eV, an isotropic optical property and excellent chemical stability. Since investigations on laser damage of this crystal by irradiation of the ArF excimer laser have been just started, elucidation of the predominant factors and mechanism of laser damage is an important issue. A small number of impurities in the crystal strongly influence the color center formation at room temperature, particularly trivalent ions such as yttrium and lanthanoid (Ln) ions. A trivalent yttrium ion is a common and persistent impurity in the $CaF_2$ single crystal because the ionic radius of $Y^{3+}$ (102 pm) is close to that of $Ca^{2+}$ (99 pm). We have reported that the time-resolved photoluminescence (PL) measurement is highly appropriate to detect a trace of Ln ions which have a close relation with degradation of $CaF_2$ single crystals because its sensitivity can be extremely enhanced by using pulsed laser light as an excitation source and the overlapping spectral components can be separated in time region.[1] Then VUV excitation bands of the PL due to a trace of Ln ions are important to discuss the reaction between the ArF laser pulses and the Ln ions. In this work, the VUV excitation bands of $CaF_2$ single crystals irradiated and unirradiated with ArF excimer laser pulses were measured at beam line BL1B at 10 K and room temperature.

## EXPERIMENTAL

Commercially available three types of $CaF_2$ single crystals, UV grade, excimer grade (A) and (B) showing yellow-green, no visible and blue PL during irradiation of ArF excimer laser, respectively, were measured. Each sample was cut into a piece with 20 mm diameter x 3 mm thickness. The 20 mm diameter surfaces were cleaved along the (111) plane and polished to an optical grade. Table 1 summarizes the impurity contents (error range is ~ 100 %) chemically analyzed by inductively coupled plasma (ICP)-mass spectroscopic method. Although there was no significant difference in iron content among any samples, the yttrium concentration in the UV grade specimen was fairly high comparing with those of the other samples. Ln ion contents of each sample were estimated as 0.1 ppm or less than 0.1 ppm.

Table 1 Chemically analyzed impurity contents (mass ppm) in the samples

| | Impurity | | | | | | | | | |
|---|---|---|---|---|---|---|---|---|---|---|
| Sample | Al | Fe | Sr | Ba | Mg | Y | La | Ce | Eu | Tb |
| Excimer grade (A) | 7 | <0.5 | 370 | 1.9 | 2 | <1 | <0.1 | <0.1 | <0.1 | <0.1 |
| Excimer grade (B) | 10 | <0.5 | 10 | 4 | 20 | <1 | <0.1 | <0.1 | <0.1 | <0.1 |
| UV grade | 1 | <0.1 | 10 | 5 | <0.2 | 5 | 0.1 | 0.1 | <0.1 | 0.1 |

## RESULTS and DISCUSSION

Before the measurements at the beam line BL1B, the transmission spectra of the samples was observed with the conventional spectrometer at room temperature. Excimer grade (A) and (B) showed no absorption after the irradiation. On the other hand, irradiated UV grade specimen showed intense absorption which was ascribed to the yttrium-associated *F* center (YFC).[1] However since the sample chamber of BL1B was baked at ~500 K for ~ 8 h in order to get the high vacuum, the defects induced by the ArF laser light were relaxed. Then transmission spectra measured at BL1B did not have the difference between irradiated and unirradiated samples. In the following paragraph, irradiated and unirradiated samples are not distinguished.

In the all samples, PL bands due to self-trapped excitons (STE) peaking at 2810 Å were observed at 10 K and room temperature. The excitation spectrum of the 2810 Å PL band and absorption spectrum observed in the UV grade specimen are showed in figure 1. These spectra were measured at ~10 K.

Weak PL of a trace of $Tb^{3+}$ peaking at 5410 Å, which was a most intense band among the PL bands due to f-f transition of $Tb^{3+}$ and a potential index for estimation of laser toughness, was observed in the UV grade specimen at ~10 K. Figure 2 shows the excitation spectrum of the 5410 Å PL band. Excitation bands were observed at 3300 Å and around 1930 Å. The signals were so weak that the life time of the PL peaking at 5410 Å was not able to be measured. These results suggests that the defects (YFC) were generated via one photon (1930 Å pulse) absorption and the STEs were generated via two photon (1930 Å pulse) absorption, as reported in the previous paper.

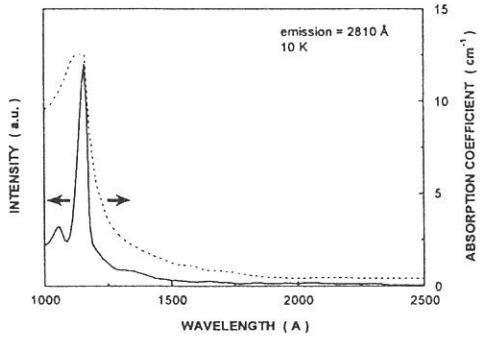


Fig.1 Absorption and Excitation Spectrum ( Emission = 281 nm ) observed in UV grade.

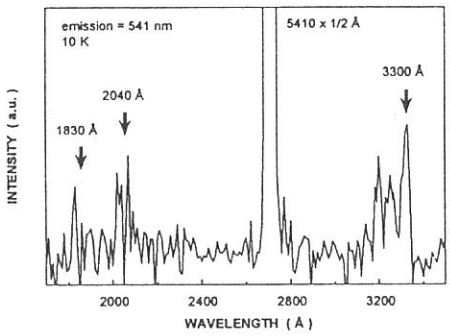


Fig. 2 Excitation Spectrum of $Tb^{3+}$ observed in the UV grade.

## REFERENCE

[1] M. MIZUGUCHI et.al., Proc. SPIE **3424**, 60 (1998)

(BL-1B)

# Optical Absorption Spectra of $(C_2H_5NH_3)_2CdCl_4$ Single Crystal

Akimasa OHNISHI, Ken-ichi TANAKA and Takehisa YOSHINARI

*Department of Physics, Yamagata University, Yamagata 990-8560*

Recently, Ohnishi *et al.* [1] studied recombination luminescence from $(C_nH_{2n+1}NH_3)_2CdCl_4$ ; n = 1, 2 and 3 crystals with VUV lights and found the largely Stokes-shifted luminescence band at 2.50 eV under excitation into the excitonic absorption range. The result suggests strongly that the excitons created by photo-excitation in those crystals relax to the self-trapped exciton (STE) states. In the present study, the tail spectra in $(C_2H_5NH_3)_2CdCl_4$ have been measured in the temperature range from 100 K to 440 K to confirm the excitonic relaxation process.

$(C_2H_5NH_3)_2CdCl_4$ single crystals were grown at RT by evaporating the aqueous solution containing stoichiometric amounts of $C_2H_5NH_2{\cdot}HCl$ and $CdCl_2{\cdot}5/2H_2O$. Samples were cleaved in a plane perpendicular to the *c*-axis, mounted on a Cu holder of a He flow-type cryostat and then were cooled by thermal-conduction. The reflection and absorption spectra were measured using synchrotron radiation (SR) from a BL-1B beam line of UVSOR. The SR was dispersed with a 1 m Seya-Namioka monochromator of which slits were kept open to a band-pass of 0.2 nm.

Figure 1 shows the fundamental absorption spectrum of $(C_2H_5NH_3)_2CdCl_4$ single crystal at 9 K which is obtained from the Kramers-Kronig analysis of the reflection spectrum. The first exciton absorption band is observed around 6.4 eV with a shoulder at 6.2 eV, which is well fitted by two Lorentzian functions at 6.23 eV and 6.38 eV shown by dotted curves. The splitting of the two bands is 0.15 eV and is almost equal to the spin-orbit splitting of a chlorine atom. From this fact the valence bands are supposed to have strong chlorine *p*-character. No excitonic absorption band was observed at about 5.5 eV, different from the previous report.[2] As seen by broken curve, since the absorption edge spectrum measured at 9 K rises with a threshold at 5.4 eV, there should be some problem in the experimental conditions or the analytical method in the previous work.

Figure 2 shows that the low energy tails of the first exciton absorption band measured in the temperature range of 100 – 440 K are semi-logarithmically plotted by thick curves as a function of photon energy. The tail spectra for different temperatures depend exponentially on photon energy over the range of 2 – 3 orders of absorption coefficient. The extrapolated thin lines of those spectra cross at one point as shown in the figure. These features indicate that the tail spectra in $(C_2H_5NH_3)_2CdCl_4$ obey the Urbach rule, expressed by the following formula,[3]

$$\alpha = \alpha_0 \exp\left(-\sigma \frac{E_0 - E}{kT}\right), \tag{1}$$

where $\alpha$ is the absorption coefficient, $E$ is the photon energy, $\alpha_0$ and $E_0$ are constants, $T$ is the temperature, $k$ is the Boltzmann constant and $\sigma$ is the temperature dependent steepness parameter. Here, the convergence point ( $E_0$ , $\alpha_0$ ) is (6.2 eV, $5.1 \times 10^9$ $cm^{-1}$).

Temperature dependence of the steepness parameters obtained from the slope of the each straight line shown in Fig.2 is plotted by solid circles in Fig. 3. The solid curve represents the best fitted one calculated with eq. (2), [4, 5]

$$\sigma = \sigma_0 \frac{2kT}{\hbar\omega} \tanh\left(\frac{\hbar\omega}{2kT}\right), \tag{2}$$

where $\sigma_0$ is the limit of $\sigma$ at high temperatures and $\hbar\omega$ is the effective energy of the phonons interacting with the excitons. We obtained $\sigma_0$ = 0.60 and $\hbar\omega$ = 46 meV from the fitting. The value of $\sigma_0$ indicates that the

STE is stable. Therefore it is concluded that the excitons in the present system are self-trapped because of the strong exciton-phonon interaction. This conclusion is consistent with the luminescence measurement by Ohnishi *et al.*[1)]

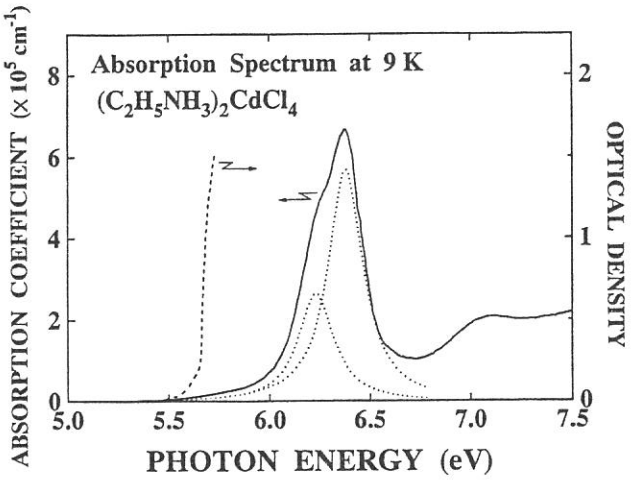


Fig. 1 Absorption spectrum of $(C_2H_5NH_3)_2CdCl_4$.

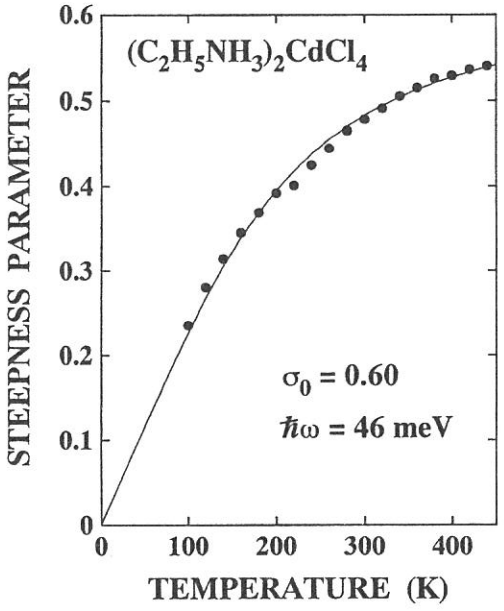


Fig. 3 Temperature dependence of the steepness parameter $\sigma$.

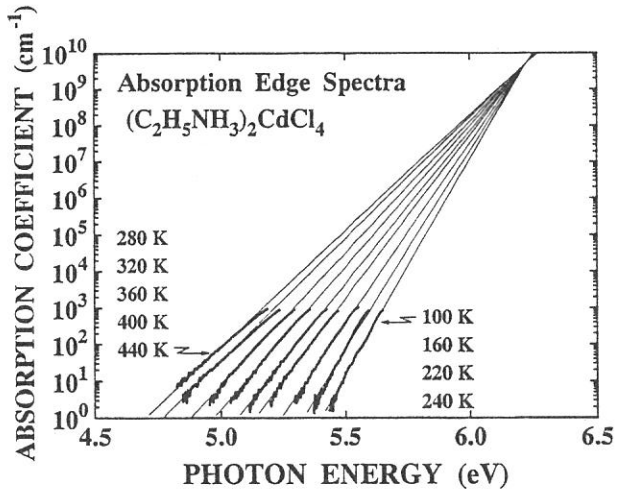


Fig. 2 Logarithmic plot of the low energy tail of the first exciton band.

## References


1) A. Ohnishi, T. Yamada, T. Yoshinari, I. Akimoto, K. Kan'no and T. Kamikawa, J. Electron Spectrosc. Relat. Phenom. **79** (1996) 163.

2) T. Yoshinari, T. Nanba, S. Shimanuki, M. Fujisawa, T. Matsuyama, M. Ikezawa and K. Aoyagi, J. Phys. Soc. Jpn. **58** (1989) 2276.

3) F. Urbach, Phys. Rev. **92** (1953) 1324.

4) H. Sumi and Y. Toyozawa, J. Phys. Soc. Jpn. **31** (1971) 342.

5) M. Schreiber and Y. Toyozawa, J. Phys. Soc. Jpn. **51** (1982) 1544.

(BL1B)

# Effects of ion implantation and thermal annealing on the photoluminescence in amorphous silicon nitride

*Kwang Soo SEOL*, Tsuyoshi FUTAMI, Takashi WATANABE, Hiromitsu KATO, and Yoshimichi OHKI*

*Department of Electrical, Electronics, and Computer Engineering, Waseda University, 3-4-1 Ohkubo, Shinjuku-ku, Tokyo 169-8555*

**Present address: Applied Laser Chemistry Lab., The Institute of Physical and Chemical Research (RIKEN), 2-1 Hirosawa, Wako-shi, Saitama 351-0198*

Category: 4. Solid- & liquid- phase spectroscopy 1 (IR, VUV, etc)

## I. EXPERIMENTAL PROCEDURES

The amorphous silicon nitride (a-$SiN_x$) film investigated in this paper was deposited on a p-type (100) silicon substrate by Low Pressure Chemical Vapor Deposition with a mixture of $SiH_2Cl_2$ and $NH_3$ gases with a pressure of 65 Pa around 700 °C. The flow rate of $NH_3/SiH_2Cl_2$ was 15 for sample A and 10 for sample B. The hydrogen content and the atomic ratio of N/Si, investigated by Rutherford back-scattering, are respectively 6 mol% and 1.52 for sample A deposited at 650 °C, and 4 mol% and 1.44 for sample B. Some films were implanted by $Ar^+$ ions with an acceleration energy of 70 keV up to a dose of $1\times10^{12}$ - $5\times10^{14}$ ions/cm$^2$. Both the as-deposited and the ion-implanted films were annealed in $N_2$ (1 atm) or in vacuum ($4.0\times10^{-2}$ Pa) by a rapid thermal annealing apparatus for 20 min.

Chemical change induced by thermal annealing was examined by Fourier-transform infrared absorption (FT-IR) and thermal desorption spectroscopy (TDS). The photoluminescence (PL) spectra were measured at room temperature using a monochromator equipped with a multichannel detector under excitation by a KrF excimer laser [wavelength: 248 nm (5.0 eV); pulse width: ~20 ns; pulse energy: ~100 mJ/cm$^2$]. The PL excitation (PLE) spectra were obtained at 77 K using synchrotron radiation (SR) at the BL1B line of UVSOR facility (Institute for Molecular Science, Okazaki, Japan). The PL lifetime was measured with a single-photon counting technique using SR at 13 K.

## II. RESULTS AND DISCUSSION

When a-$SiN_x$ film is irradiated by a KrF excimer laser, it exhibits a broad PL band centered at about 2.4 eV. The PL intensity gradually decreases and the PL peak energy shifts to a lower energy with an increase of the implanted dose of $Ar^+$ ions. From the result of the Gaussian fitting, this clearly indicates that the PL spectrum observed before ion-implantation is composed of two PL bands centered at 2.66 and 2.15 eV. The PL intensity decreases according to a power law with an increase in dose, and the exponent is larger for the 2.66 eV PL than the 2.15 eV PL. This is the reason that the PL shape shifts toward red.

In a-$SiO_2$ films, several PL bands such as the ones due to the oxygen vacancies and the non-bridging oxygen hole centers are induced by ion implantation. The intensities of these PLs become larger with an increase in implantation dose. In some a-$SiO_2$ films such as the one synthesized by plasma-enhanced chemical vapor deposition or the method called SIMOX (Separation by IMplanted OXygen), these PLs are seen without ion implantation. From these results, the PLs are considered to be associated with oxygen-deficient or oxygen-rich defects and that the ion implantation has an action of manifesting weak sites such as strained bonds by converting them into PL-detectable defects. However, the PL observed in the present study decreases its intensity with an increase of implanted dose of ions. This is the exact opposite of the result of a-$SiO_2$. Therefore, the PL in a-$SiN_x$ is considered not to be due to implantation-induced defects such as vacancies or bond-breaks.

The two PL bands that had been quenched by ion-implantation are recovered by thermal annealing done at 900 °C for 20 min in $N_2$. But the recovered intensity is about one third of the intensity before ion-implantation. In a-$SiO_2$, the increased intensity by ion-implantation decreases by similar thermal annealing. This is also the opposite result of the present case of a-$SiN_x$.

The PL intensities of the 2.66 and 2.15 eV bands observed in non-implanted sample decrease abruptly by thermal annealing in vacuum at temperatures above 700 °C. Figure 1 shows the PL decay excited by 5.0 eV photons from SR, observed in the as-deposited sample A. It is clear that the decay is expressed by a stretched exponential function,

$$I(t)\propto(\tau/t)^{1-\beta}\exp\{-(t/\tau)^{\beta}\},$$

where $I$ is the PL intensity, $t$ the time, $\tau$ the effective lifetime, and $\beta$ is a parameter which has a value between 0 and 1. When this sample is thermally annealed in vacuum, $\tau$ decreases at above 700 °C, which $\beta$ hardly changes.

From the result of FT-IR, it is clear that the absorption at 3340 $cm^{-1}$ due to N-H bonds and the one at 2200 $cm^{-1}$ due to Si-H bonds abruptly decrease by thermal annealing at temperatures above 700 °C. Both the 2.66 and 2.15 eV PL bands clearly show a linear relationship with the hydrogen-related bonds. The above IR result indicates that hydrogen is released by the annealing. From the measurement of TDS, it is confirmed that the desorption of hydrogen starts around 700 °C.

The above-mentioned results suggest that the PL is related to the desorption of hydrogen. Therefore, the non-implanted sample A was thermally annealed at 900 °C for 20 min in vacuum or in 100 % hydrogen at 1 atm, and PL spectra were observed. While no change is seen for the $H_2$ annealing, the PL intensity decreases significantly by the vacuum annealing. This clearly supports the above assumption that the PL in $SiN_x$ is related to hydrogen desorption.

Shown in Fig. 2 are the PL excitation spectra of sample A monitored at 2.66 and 2.15 eV, measured at 77 K using SR. It is clear that the PL bands are excited by the photons with energies above 4.5 eV. The energy of 4.5 eV is close to the value of optical band gap for the near-stoichiometric $SiN_x$. Therefore, the PL bands are considered to be related to recombination of electrons and holes, generated by interband photon absorption.

Previous studies reported several PL bands between 1.8 and 4.0 eV in near-stoichiometric or silicon- or nitrogen-rich a-$SiN_x$. Among those, a broad PL centered around 2.5 eV is commonly observed in near-stoichiometric or nitrogen-rich $SiN_x$. Based on the fact that the peak energy of the PL is similar to the calculated energy between the state of silicon dangling bond and valence or conduction band edge, the PL was previously attributed to the radiative recombination at the silicon dangling bond. However, the present results suggest that the PL is not due to implantation-induced defects, and that the PL intensity decreases if hydrogen is released. Furthermore, the properties of the PL observed in the present study are very similar to those of the PL observed in hydrogenated amorphous silicon (a-Si:H). In a-Si:H, the PL intensity also decreases if hydrogen is desorbed. The reason for this is considered that hydrogen in a-Si:H effectively eliminates the non-radiative sites relating to Si dangling bonds. Furthermore, the PL in a-Si:H is quenched by ion-implantation that could easily break Si-H bonds and Si-Si regular bonds. This similarity suggests that the ion-induced defects such as Si dangling bonds are not the origin of PL in a-$SiN_x$ but non-radiative recombination centers that quench the PL. Hydrogen is thought to eliminate the recombination centers.

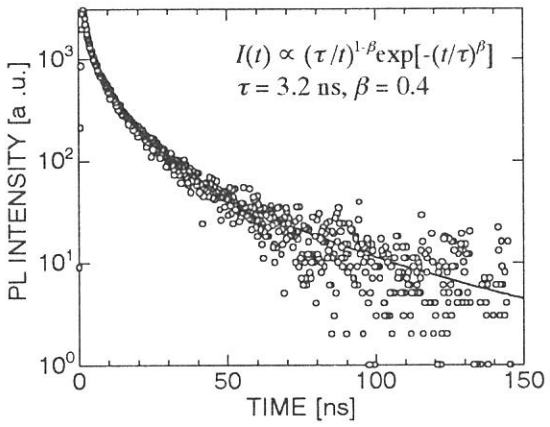


Fig. 1 PL decay excited by 5.0 eV photons from SR observed in the as-deposited sample A. $I$ is the PL intensity, $t$ the time, $\tau$ the effective lifetime, and $\beta$ is a parameter which has a value between 0 and 1.

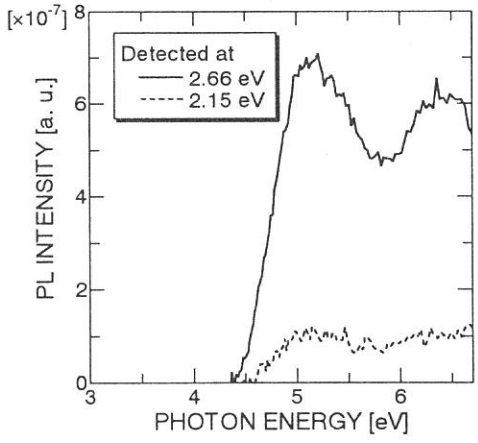


Fig. 2 PL excitation spectra for the 2.66 and 2.15 eV PL bands observed in sample A.

(BL1B)

# Optical Spectra of $PbF_2$ Crystals in the VUV Region

Masami FUJITA, Minoru ITOH [A], Jun-ichi MURAKAMI [A],
Hideyuki NAKAGAWA [B], Mamoru KITAURA [C] and Dmitri L. ALOV [D]

*Maritime Safety Academy, Wakaba, Kure 737-8512*
[A] *Department of Electrical and Electronic Engineering, Faculty of Engineering, Shinshu University, Wakasato, Nagano 380-8553*
[B] *Department of Electrical and Electronics Engineering, Faculty of Engineering, Fukui University, Bunkyo, Fukui 910-8507*
[C] *Fukui National College of Technology, Geshi, Sabae 916-8507*
[D] *Institute of Solid State Physics, Chernogolovka, Moscow 142432 Russia*

Lead fluoride is an interesting material because it has two structural modifications which coexist at normal conditions. The orthorhombic phase ($\alpha$-$PbF_2$) is more stable below 320℃, but the cubic phase ($\beta$-$PbF_2$) is also metastable at low temperatures. Optical spectra of $\beta$-$PbF_2$ have been measured previously using polished surface and evaporated film[1], because flat surface cannot be obtained by the cleavage of the crystal. It is known that the phase transition of $\beta$-$PbF_2$ into $\alpha$ phase is caused by application of pressure. In the present experiment, reflection spectra of $\alpha$- and $\beta$-$PbF_2$ have been measured in order to study the effect of surface treatment on the optical spectra and to investigate the electronic structure of $Pb^{2+}$ $5d$ core exciton state in lead fluoride.

Single crystals of $\alpha$-$PbF_2$ were grown from aqueous solution. Reflection spectra were measured using the as-grown surface which contains the *ab*-plane. Single crystals grown by the Bridgman method were used for the measurement of $\beta$-$PbF_2$. Experiments were performed at BL1B of UVSOR.

Reflection spectra of $\alpha$-$PbF_2$ crystal at low temperature are shown in Fig. 1(a) for $E//a$ and $E//b$ polarization. Figure 1(b) and (c) show the reflection spectra of $\beta$-$PbF_2$ for a polished surface and for a cleaved surface, respectively. The peak at 5.7 eV in each spectrum is due to the lowest exciton transition. The exciton band in Fig. 1(a) exhibits dichroism and the exciton band in Fig. 1(c) has three fine structures[2]. It was found that the spectral shape of the exciton band in Fig. 1(b) can be fitted well by the average of the spectra for $E//a$ and $E//b$ in Fig. 1(a). The spectrum in the 6-7 eV region in Fig. 1(b) exhibits intermediate features between Fig. 1(a) and (c). These facts indicate that the phase transition on the surface of cubic crystal into orthorhombic phase is induced by the stress during mechanical polishing. We regard the spectrum of the cleaved surface as intrinsic to $\beta$-$PbF_2$.

Figure 2 shows reflection spectra of $\alpha$- and $\beta$-$PbF_2$ up to 30eV. In the 10-18eV region,

several sharp peaks are observed in $\beta$-$PbF_2$, while broad structures are observed in $\alpha$-$PbF_2$. The structures below 18 eV are attributed to the transitions from both $F^-$ $2p$ valence band and $Pb^{2+}$ $6s$ valence band. Sharp peaks observed in the 20-25eV region are due to the exciton transition from $Pb^{2+}$ $5d$ core level to the $6p$ level. The peaks 1, 2 and 3 are assigned to the transitions from $^1S_0$ ground state to the $J$=1 excited states of $^3P_1$, $^1P_1$ and $^3D_1$, as is the case of $PbCl_2$ and $PbBr_2$[3]. In addition to these main peaks, a small peak 0 is observed in both crystals and a peak 3' is observed in $\beta$-$PbF_2$. Some of the $J\neq1$ excited states, which are optically forbidden in a free-ion state, can couple with the $J$=1 states through the crystal-field potential in each crystal. The additional peaks 0 and 3' are probably due to the transitions to such excited states. The appearance of these peaks in $\beta$-$PbF_2$ indicates that the crystal-field interaction in $Pb^{2+}$ $5d$ core level plays an important role as is the case of $Tl^+$ $5d$ core exciton in thallous halides[4], because the cubic crystal-field does not lift the degeneracy of $6p$ orbitals.

## References


[1]J. H. Beaumont, A. J. Bourdillon and J. Bordas: J. Phys. C Solid State Phys. **10**(1977)761.

[2]M. Fujita, M. Itoh, H. Nakagawa, M. Kitaura and D. L. Alov: J. Phys. Soc. Jpn. **67**(1998)3320.

[3]M. Fujita, H. Nakagawa, K. Fukui, H. Matsumoto, T. Miyanaga and M. Watanabe: J. Phys. Soc. Jpn. **60**(1991)4393.

[4]M. Fujita, N. Ohno, Y. Kiyama and K. Nakamura: J. Electron Spectrosc. Relat. Phenom. **79**(1996)59.


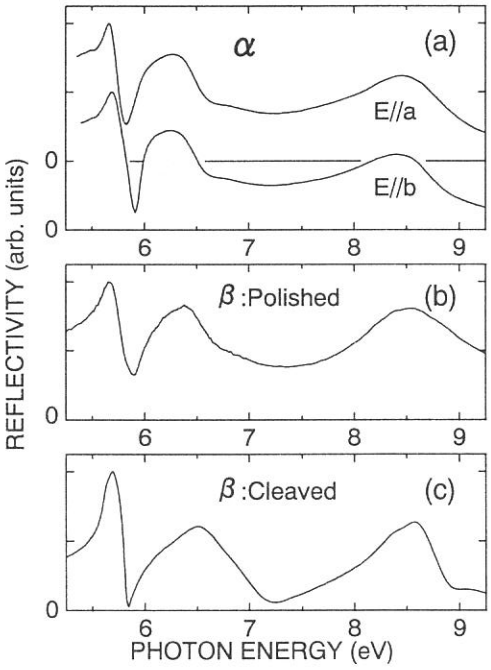


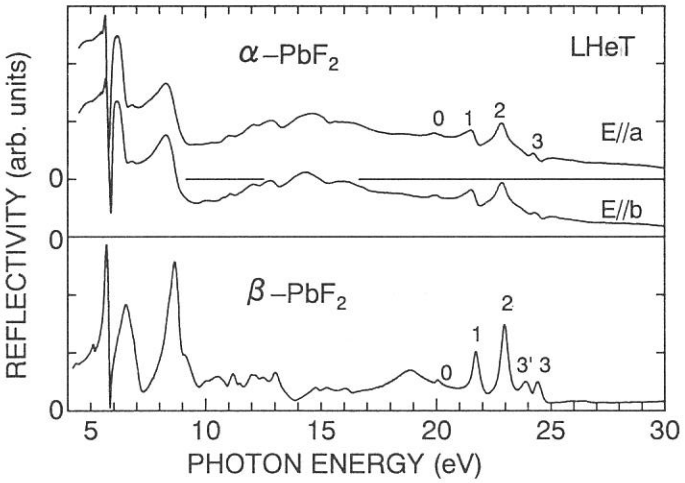


Fig. 2. Reflection spectra of $\alpha$- and $\beta$-$PbF_2$ crystals in the 5-30 eV region.

Fig. 1. Reflection spectra of (a) $\alpha$-$PbF_2$, (b) $\beta$-$PbF_2$ with polished surface and (c) $\beta$-$PbF_2$ with cleaved surface.

(BL1B)

# Far-Infrared to Vacuum-Ultraviolet Reflectivity Spectrum of $La_{0.70}Sr_{0.30}MnO_3$: Evidence Against Small Drude Weight

Koshi TAKENAKA,* Suguru KASHIMA, and Shunji SUGAI

*Department of Physics, Nagoya University, Chikusa-ku, Nagoya 464-8602*

Optical reflectivity study can make an essential role in the both fundamental and practical researches on the double-exchange ferromagnetic-metal manganites showing "colossal magnetoresistance (CMR)" because it enables us to not only deduce dielectric functions but also examine separately two key-elements of charge transport – carrier density (or Drude weight) and scattering time. The charge transport is one of the central concerns among the both studies.

The previous reflectivity studies on $La_{1-x}Sr_xMnO_3$ [1] have revealed the outline of the systematic change of the electronic structure with Sr-substitution. One of the significant implications is such small Drude weight that we cannot attribute it to mass-enhancement. However, the origin or truth of the small Drude weight is not well-investigated because the experiments did not cover the sufficient energy region or/and did not have the sufficient accuracy. We report here the established optical reflectivity spectrum $R(\omega)$ of $La_{0.70}Sr_{0.30}MnO_3$ measured on the *cleavage* surface of single crystal for a wide energy range (0.005−40 eV). The present result demonstrates that the small Drude weight originates from the distortion of the spectrum caused by the damages introduced into the surface by polishing and the true Drude weight is large and consistent with the Hall effect [2] and specific heat studies [3].

Single crystals of $La_{0.70}Sr_{0.30}MnO_3$ were grown by a floating zone method. The Curie temperature $T_C$=362 K. In order to obtain defect-free surfaces we cleaved the single-crystalline rod. Near-normal incident reflectivity measurements were made using a Fourier-type interferometer (0.005-2.2 eV), a grating spectrometer (1.2-6.5 eV), and a Seya-Namioka type spectrometer for vacuum-ultraviolet synchrotron radiation (4.0-40 eV) at BL1B of the UVSOR facility, Institute for Molecular Science. All data were taken at room temperature.

We show in Fig. 1 the reflectivity spectrum of $La_{0.70}Sr_{0.30}MnO_3$ measured on the cleavage surface of single crystal (solid line). It is characterized by a sharp edge at about 1.6 eV and a large weight below it. The implication of the reflectivity data becomes clearer when the optical conductivity spectrum is deduced via the Kramers-Kronig transformation of the reflectivity data. The optical conductivity spectrum exhibits a pronounced Drude-like component with large spectral weight below the edge (solid line in Fig. 2).

The main purpose in this study is the precise estimation of the "Drude weight". In a simple Drude model, $N^*_{\rm eff}(\omega_{\rm ps})=n(m_0/m^*)$, where $N^*_{\rm eff}(\omega)$ is the effective carrier number defined as

$$N^*_{\rm eff}(\omega) = \frac{2m_0V}{\pi e^2}\int_0^{\omega}\sigma(\omega')d\omega' \qquad (1)$$

($n$: carrier number per Mn-atom; $m_0$: a bare electron mass; $m^*$: effective mass; $\omega_{\rm ps}$; plasma frequency; $V$: the volume per Mn-atom). $N^*_{\rm eff}(\omega_{\rm ps})$ is so-called Drude weight. It is difficult, however, in the present case to estimate Drude weight because a simple Drude model seems not valid; the decay rate is too slow compared with $\propto\omega^{-2}$ to be interpreted within the Drude model.

However, the present result clearly demonstrates at least the following fact that the Drude weight is much larger than that previously reported [1]. For example, we assume $\omega_{ps}$=1.6 eV (reflectivity edge), then $N^*_{eff}(\omega_{ps})$=0.346. Using $n\sim1$ per Mn-atom estimated from Hall effect study [2], mass-enhancement $m^*/m_0$ is estimated to be 2.9, which is consistent with the result of specific heat measurement [3].

The discrepancy to the previous result originate from the damages of the sample surface introduced by polishing. In Fig. 1 is shown also the reflectivity spectrum measured on the surface polished with diamond powder of diameter 0.3 $\mu$m (dashed line). It is found that polishing distorts drastically $R(\omega)$ of $La_{0.70}Sr_{0.30}MnO_3$. The previous data by Okimoto *et al.* [1] resembles closely this distorted spectrum. The damage of the surface probably localizes the carriers. However, as the wavelength of the incident light becomes longer, light reaches the inner, not damaged part, and hence $R(\omega)$ recovers the true spectrum, which is consistent with that the discrepancy almost disappears below 0.03 eV. "Small Drude weight" originates from the above restoration process (dashed line of Fig. 2).

The authors would like to thank Professor M. Kamada and Dr. M. Hasumoto for the useful advice and skillful technical assistance to use SOR beam. They are also grateful to Professor Y. Moritomo for many discussions and for the help in the visible-ultraviolet spectroscopy.

References

* Electronic address: k46291a@nucc.cc.nagoya-u.ac.jp

[1] Y. Okimoto *et al.*, Phys. Rev. B **55**, 4206 (1997).
[2] A. Asamitsu and Y. Tokura, Phys. Rev. B **58**, 47 (1998).
[3] J. M. D. Coey *et al.*, Phys. Rev. Lett. **75**, 3910 (1995).

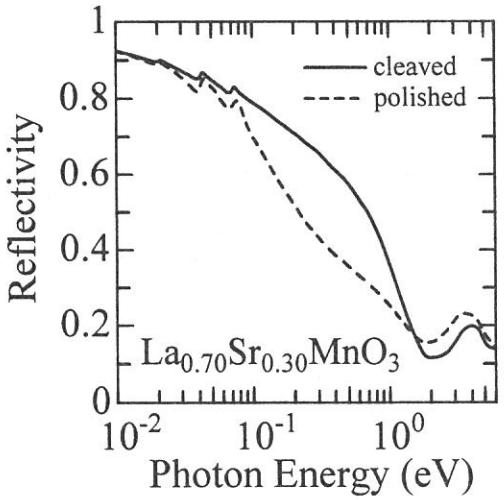


FIG. 1 Optical reflectivity spectra of $La_{0.70}Sr_{0.30}MnO_3$ measured on the cleavage surface (solid line) and the polished surface (dashed line).

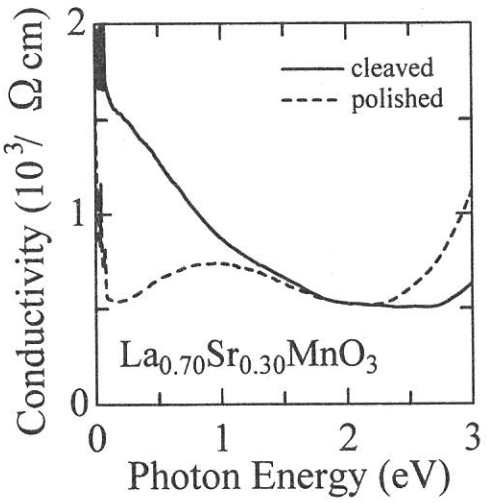


FIG. 2 Optical conductivity spectra of $La_{0.70}Sr_{0.30}MnO_3$ deduced from the reflectivity spectra measured on the cleavage (solid line) and polished (dashed line) surfaces via Kramers-Kronig transformation.

(BL1B)

# Reflection Spectra of Hydrogen-Bonded Ferroelectrics $PbHPO_4$ and $PbHAsO_4$

Noriaki KIDA, Nobuhito OHNO and Masao KAMADA[A]

*Division of Electronics and Applied Physics, Graduate School of Enginnering*
*Osaka Electro-Communication University, Neyagawa 572-8530, Japan.*
*[A] UVSOR Facility, Institute for Molecular Science, Okazaki 444-8585, Japan.*

Lead monohydrogen phosphate $PbHPO_4$ (LHP) and its isomorphs $PbHAsO_4$ (LHA) are quasi-one dimensional ferroelectrics that have been classified as a second order structural phase transition from a monoclinic with a space group $Pc$ to a paraelectric $P2/c$ at $T_C$=310 K and 312 K, respectively. The $PO_4$ or $AsO_4$ tetrahedra in both materials are linked to linear chains by short O-H-O bonds and not cross-linked to one another, in contrast to well studied $KH_2PO_4$ (KDP). This simple crystal structure has been taking an appeal to many researchers as a reference material to understanding of proton ordering in hydrogen-bonded ferroelectrics.

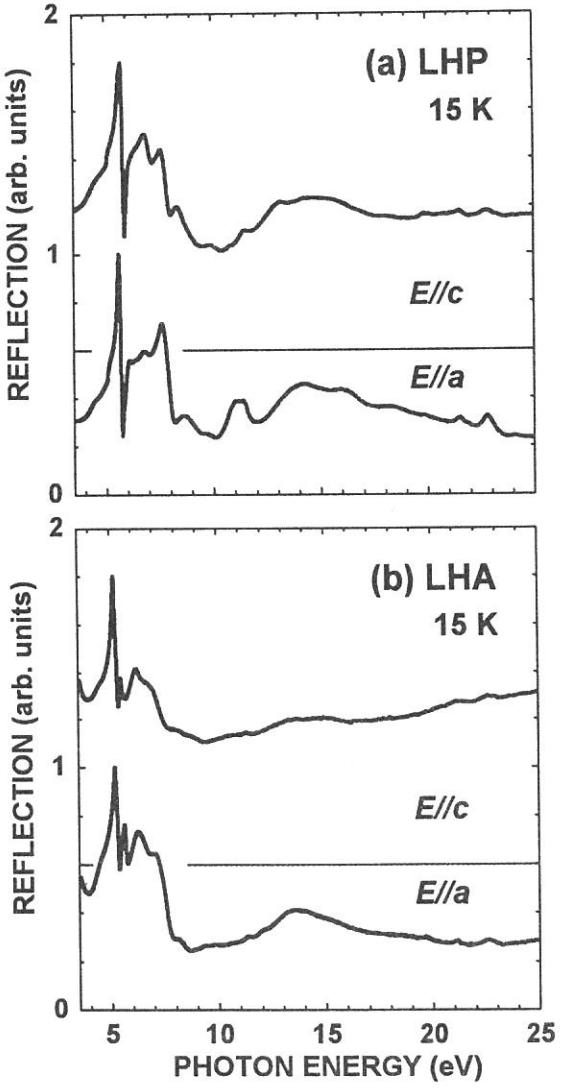


Figure 1. Polarized reflection spectra of (a) LHP and (b) LHA for E//a and E//c at 17 K.

In the present study, reflection spectra of single crystals of LHP and LHA have been investigated for the first time in the VUV region up to 25 eV by using polarized synchrotron radiation at BL1B beamline.

The specimens of LHP and LHA grown from the conventional gel-growth method [1] were used for optical measurements.

Figure 1 shows the reflection spectra of a single crystals of (a) LHP and (b) LHA for polarization parallel to the crystallographic $a$-axis ($E//a$) and the $c$-axis ($E//c$), respectively, measured at 17 K. The direction of $P_S$ is in the $ac$ plain, close to the $a$-axis. Distinguished sharp peaks with dispersive structure are observed at the absorption edge at 5.62 eV for $E//a$ and at 5.77 eV for $E//c$ in LHP. In LHA, these structures are located at 5.14 eV for $E//a$ and at 5.18 eV for $E//c$. They could be assigned as the first exciton transitions. The polarized reflection spectra of KDP and $KH_2AsO_4$ (KDA) have been reported [2, 3]. The reflection peaks of KDP and KDA at the absorption edge are observed at 8.2 and 7.0 eV, respectively, which have been ascribed to the transitions mainly due to the anions. No exciton transition is observed at the absorption edge in KDP and KDA. Therefore, we deduce the lowest transition of LHP and LHA as due to cationic excitation in $Pb^{2+}$; the upper valance bands are mainly composed of $Pb^{2+}$ $6s$ states, and the lowest conduction bands are $Pb^{2+}$ $6p$ states in its origin.

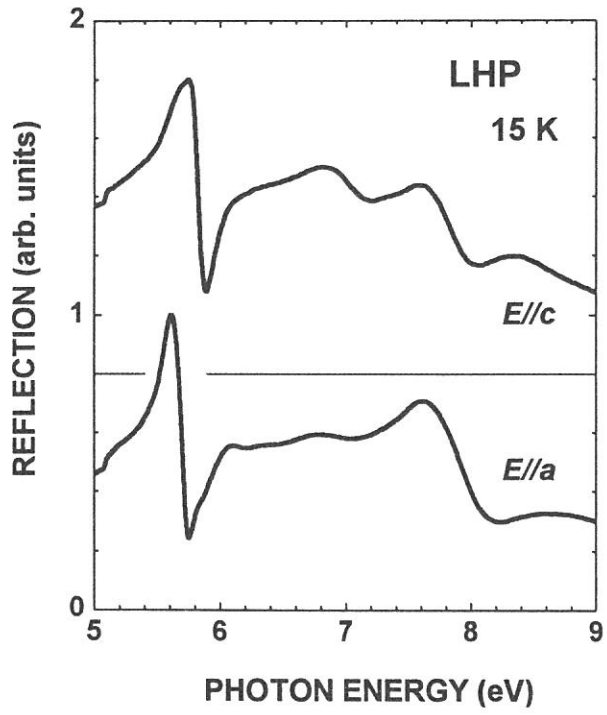


Figure 2. Expanded views of the reflection spectra near the first direct exciton region of LHP for $E//a$ and $E//c$ at 15 K.

Figure 2 shows expanded view of the reflection spectra of LHP near the first direct exciton region at 15 K. A clear shoulder structure at higher energy side of first direct exciton transtion is observed for $E//a$ at 6.0 eV for LHP. We tentatively assigned it to the $n$=2 state of exciton Rydberg series that permits an estimate of the binding energy ($E_b$) of the exciton. We obtain $E_b \simeq 670$ meV, which is comparable with $E_b$=680 meV for the first exciton of $\beta$-$PbF_2$ [4]. However, recent experimental investigation for $\beta$-$PbF_2$ shows that such a $n$=2 exciton structure is not observed [5]. Bands around 7 eV are attributed to the transition from the valence band to the conduction bands, which are mixed by the spin-orbit interaction of Pb ions. With increasing of temperature, the first direct excition transition is shift to low energy side and visible even above $T_C$, indicating that the excitions are stable in paraelectric phase of LHP and LHA.

Sharp peaks at 21.7 eV and 22.9 eV are observed in LHP at 15 K, which may attribute to the $Pb^{2+}$ $5d$ core excitons as observed in the lead halides [6, 7]. In LHA, these structures are barely discernible. Their energy positions are close to $^3P_1$ and $^1P_1$ levels of the free $Pb^{2+}$ ion. Preliminarly experiment on the photoelectoron spectroscopy of LHP using Al $K_\alpha$ radiation at 300 K indicates that the $Pb^{2+}$ $5d_{3/2}$ and $5d_{5/2}$ levels are located at ~22 and ~25 eV below the top of the valance band. An estimate of the core exciton binding energies is ~5 eV for $^3P_1$ state and ~8 eV for $^1P_1$ state. These values are comparable with that of $\beta$-$PbF_2$ [4]. Further analysis of electronic strucutures is now in progress.

We thank Prof. K. Deguchi for kindly providing single crystals of LHP and LHA.

[1] K. Deguchi, *J. Phys. Soc. Jpn.* **65**, 4076 (1996).

[2] S. Saito and R. Onaka, *Ferroelectrics* **21**, 553 (1978).

[3] S. Matsumoto, M. Fujisawa and S. Suga, *J. Electron Spectrosc. Relat. Phenom.* **79**, 51 (1996).

[4] J. H. Beaumont, A. J. Bourdillon and J. Bordas, *J. Phys. C: Solid State Phys.* **10**, 761 (1977).

[5] M. Fujita, M. Itoh, H. Nakagawa, M. Kitaura and D. L. Alov, *J. Phys. Soc. Jpn.* **67**, 3320 (1998).

[6] T. Hayashi, K. Toyoda and M. Itoh, *J. Phys. Soc. Jpn.* **57**, 1861 (1988).

[7] M. Fujita, H. Nakagawa, K. Fukui, H. Matsumoto, T. Miyanaga and M. Watanabe, *J. Phys. Soc. Jpn.* **60**, 4983 (1991).

(BL1B)

# Reflection Spectra of Oriented Polyethylene Terephthalate Films in the Ultraviolet and Vacuum Ultraviolet Regions

Isuke OUCHI, Ikuo NAKAI[A], Masao KAMADA[B], Shin-ichiro TANAKA[B] and Masami HASUMOTO[B]

*Faculty of Engineering, Tokushima Bunri University, Shido, Kagawa 769-2193*
*[A] Faculty of Engineering, Tottori University, Koyama, Tottori 680-8552*
*[B]Institute for Molecular Science, Myodaiji, Okazaki 444-8585*

Ultraviolet spectra of polyethylene terephthalate (PET) have been studied in detail by one of the authors[1] and other researchers[2] since long ago; core electron spectra of this polymer have also been examined by ourselves[3,4] and others.[5,6] However, the photo absorption of valence electrons in the deeper levels have not been reported except some by XPS.[7,8] The purpose of the present study is to investigate the deeper electronic structure of PET by use of ultraviolet and vacuum ultraviolet absorption of synchrotron radiation, whose polarized nature makes it possible to examine the effect of molecular orientation and helps to determine the character of the energy levels.

In the actual measurements, reflection spectra of thick films were taken and their Kramers-Kronig conversion was made to obtain the absorption spectra. PET films are very transparent in the visible region but absorb light strongly in the ultraviolet region; in the previous study[1], films as thin as 0.1 $\mu$ m was utilized for the measurement of ultraviolet absorption but these are not thin enough for the measurement in vacuum ultraviolet region. On the other hand, it was proven there that the Kramers-Kronig conversion of reflection spectra of thick films gave rise to almost identical absorption spectra as directly measured by transmission method by use of the thin film.

We utilized the 1m Seya-Namioka type monochromator installed at the BL-1B of UVSOR. Five pieces of film samples were fixed on a copper plate, which was then attatched to the holder; the sample chamber was evacuated overnight before the measurement. The incidence angle was set as 12.5°. Actual measurements were made between 500A and 6000A.

Thick PET films were obtained from the Film Research Laboratory of Teijin Limited: amorphous undrawn films of 100 $\mu$ m thickness, uniaxially drawn films of 60 $\mu$ m and biaxially drawn films of 100 $\mu$ m.

An example of the reflection spectra is shown in Fig. 1; this spectrum is already corrected for multiple reflection. The method of the correction was taken from Kato[9] and was the same as the previous paper.[1]

The phase of reflected light was calculated from the reflection spectra by the Kramers-Kronig relation; contributions from the outside of the measured wavelength region were calculated by use of Roessler's approximation[10] as in the previous work.[1]

Using Fresnel equations, diffractive index, extinction coefficients and absorption coefficients were calculated. Examples of absorption spectra obtained in this way are shown in Fig, 2.

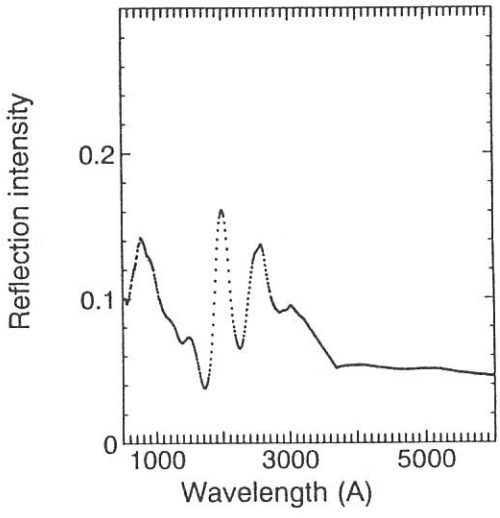


Fig. 1. Reflection spectra of an undrawn PET film. Multiple scattering is already corrected.

In the absorption spectrum of an undrawn PET film, which is shown in Fig. 2 (a), there are absorption peaks at 300 - 290 nm (4.13 - 4.26 eV), 254 - 244 nm (4.88 - 5.09 eV), 197 nm (6.29 eV), 145 nm (8.55 eV) and 91 - 83 nm (13.6 - 14.9 eV) with a broad shoulder at around 120 nm (ca.10.5 eV). The first three peaks in the ultraviolet region are the same as reported before and correspond to $^1A_g \rightarrow {}^1B_u$ transitions; according to Pariser-Parr-Pople approximation, the third peak at 197 nm consisted of two peaks of opposite polarity.[1] The absorption spectrum of a biaxially drawn PET film is displayed also in Fig. 2 (a). A slight disagreement in the peak positions must be due to technical handlings; negative absorption is also due to poor handling in some approximation and corrections, which must be improved.. The nature of the peaks at smaller wavelengths is also still to be studied.

Fig. 2 (b) shows the spectra of an uniaxially drawn PET film; their molecular orientation is either parallel or perpendicular to the electric vector of incident light and the dichroic nature is very clear. The double peak at 300 - 290 nm and a large peak at the shortest wavelength are of ⊥ polarity, the peak at 254 - 244 nm is very strongly polarized along ∥ direction, the other two are slightly ∥ polarized. Those in the longer wavelengths region agree to the previous result.1)

Relative resemblance of the spectral shape between a biaxially drawn film and an uniaxially drawn film with its draw axis parallel to the electric vector of the incident light, and also between an undrawn film and an uniaxially drawn film with perpendicular direction may be understandable from the structure change of the film by means of the stretching and heat-treatment. This, however, is still to be examined.

The authors are indebted to Mr. N. Takagi, Film Research Laboratory, Teijin Limited, who kindly sent us the film samples.

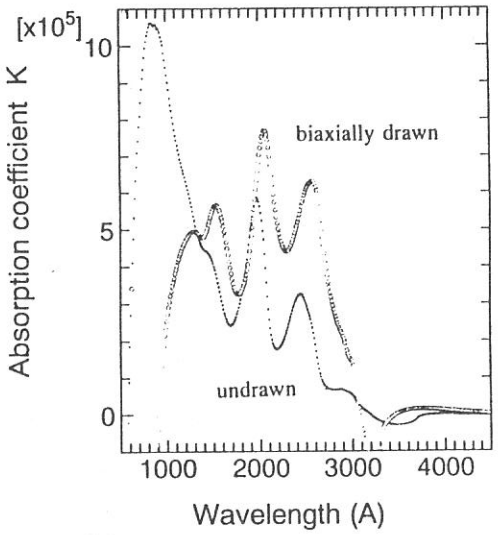


Fig. 2 (a) Converted absorption spectra of undrawn and biaxially drawn PET films.

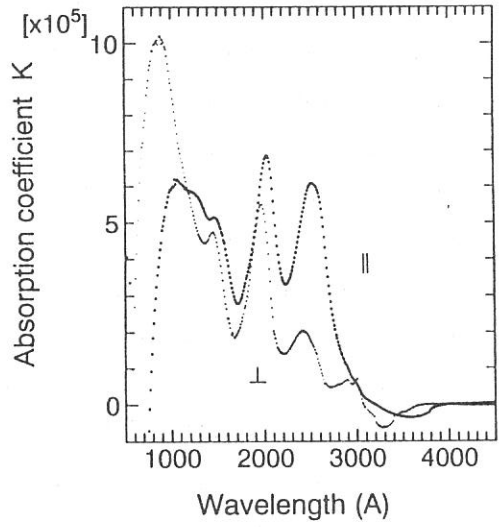


Fig. 2(b). Converted absorption spectra of an uniaxially drawn PET films. The symbols ∥ and ⊥ mean that the drawing direction is parallel or perpendicular to the electric vector of incident light, respectively.

1) I. Ouchi, Polym. J., 15 (1983) 225. 2) J.P. LaFemina and G. Arjavalingam, J. Phys. Chem., 95 (1991) 984. 3) I. Ouchi et al., Polym. J., 27 (1995) 127. 4) I. Ouchi et al., J. Electr. Spectr. Rel. Phenom., 78 (1996) 363. 5) E.G. Rightor et al., J. Phys. Chem., B 101 (1997) 1950. 6) S.G. Urquhart et al., ibid. 2267. 7) M. Chtaib et al., Phys. Rev. B, 44 (1991) 10816. 8) P. Boulanger et al., J. Electr. Spectr. Rel. Phenom., 63 (1993) 53. 9) R. Kato, J. Phys. Soc. Jpn., 16 (1961) 2525. 10) D.M. Roessler, Brit. J. Appl. Phys., 16 (1965) 1119.